Epoxide pathways improve model predictions of isoprene markers and reveal key role of acidity in aerosol formation

Havala O. T. Pye,[*,†] Robert W. Pinder,[†] Ivan R. Piletic,[†] Ying Xie,[†,‡] Shannon L. Capps,[†] Ying-Hsuan Lin,[¶] Jason D. Surratt,[¶] Zhenfa Zhang,[¶] Avram Gold,[¶] Deborah J. Luecken,[†] William T. Hutzell,[†] Mohammed Jaoui,[§] John H. Offenberg,[†] Tadeusz E. Kleindienst,[†] Michael Lewandowski,[†] and Edward O. Edney[†]

US Environmental Protection Agency, National Exposure Research Laboratory, Research Triangle Park, North Carolina, USA, Shanghai Meteorological Service, Shanghai, China, University of North Carolina at Chapel Hill, Department of Environmental Sciences and Engineering, Chapel Hill, North Carolina, USA, and Alion Science and Technology, Box 12313, Research Triangle Park, North Carolina, USA

E-mail: pye.havala@epa.gov

Abstract

Isoprene significantly contributes to organic aerosol in the southeastern United States where biogenic hydrocarbons mix with anthropogenic emissions. In this work, the Community Multiscale Air Quality model is updated to predict isoprene aerosol from epoxides produced under

[*]To whom correspondence should be addressed
[†]US Environmental Protection Agency
[‡]now at: Shanghai Meteorological Service
[¶]University of North Carolina at Chapel Hill
[§]Alion Science and Technology

both high- and low-NO_x conditions. The new aqueous aerosol pathways allow for explicit predictions of two key isoprene-derived species, 2-methyltetrols and 2-methylglyceric acid, that are more consistent with observations than estimates based on semivolatile partitioning. The new mechanism represents a significant source of organic carbon in the lower 2 km of the atmosphere and captures the abundance of 2-methyltetrols relative to organosulfates during the simulation period. For the parameterization considered here, a 25% reduction in SO_x emissions effectively reduces isoprene aerosol while a similar reduction in NO_x leads to small increases in isoprene aerosol.

Introduction

$PM_{2.5}$ (particles with aerodynamic diameters of 2.5 μm or less) is a criteria pollutant with implications for public health and climate. Organic aerosol resulting from complex interactions of various emission sources significantly contributes to $PM_{2.5}$ (*1*). The spatial, seasonal, and temperature trends in aerosol optical thickness over the eastern United States indicate a significant role for biogenic secondary organic aerosol (SOA) (*2*); additionally, more than half of aerosol carbon is modern (vs. fossil) in origin for a variety of locations (*3*, *4*), which is consistent with a biogenic hydrocarbon source.

Isoprene, the most abundant non-methane hydrocarbon emitted (*5*), is likely a large contributor to organic aerosol, particularly in the southeastern United States. Organic carbon (OC) model underestimates such as those in the Community Multiscale Air Quality (CMAQ) model (*6*) may arise from an underrepresentation of isoprene aerosol pathways. Isoprene-derived compounds detected in ambient aerosol, including 2-methyltetrols, 2-methylglyceric acid (2-MG), and organosulfates account for 19.4% of organic aerosol in the work of Lin et al. (*7*). When adjusted to total OC using laboratory-based ratios, 12-29% of total OC is attributable to isoprene (*8–10*). Methyltetrols are likely the most abundant individual isoprene SOA constituents and have been found to account for up to 6.6% of OC in Centreville, Alabama (*11*), and 5.2-8.9% of total organic aerosol in Yorkville, Georgia (*7*). Factors derived from positive matrix factorization (PMF) of aerosol mass spectrom-

eter (AMS) data have been linked with isoprene SOA and captured as much as 53% and 33% of organic aerosol in Borneo (*12*) and Atlanta, Georgia (*13*) respectively. Modeling studies further support a significant role for later generation isoprene products in forming OC (*14*, *15*).

Traditionally, isoprene SOA has been represented using an Odum 2-product approach (*16*, *17*) based on vapor pressure dependent partitioning of semivolatile surrogates. However, both particle water and organics likely serve as partitioning phases (*18*), and comparisons of the modern and fossil portions of water soluble organic carbon (WSOC) and total OC indicate that biogenic OC is preferentially present in the aqueous phase in the eastern United States (*19*). Furthermore, known isoprene SOA constituents like the 2-methyltetrols are highly correlated with WSOC in the southeastern U.S. (r^2 of 0.88 in Centreville, Alabama (*11*)). While both cloud and aerosol water are candidates for water-soluble organic partitioning, McNeill et al. indicate that aqueous-phase aerosol processing may result in more OC than in-cloud processing as a result of more concentrated conditions (*20*).

Later generation isoprene products with the potential to form SOA have been identified, but are not yet widely incorporated into models. Under low-NO_x conditions in which isoprene peroxy radicals ($RO_2\cdot$) react predominantly with hydroperoxal radicals ($HO_2\cdot$), isoprene epoxydiols (IEPOX) are formed with a relatively high yield (*21*). Under high-NO_x conditions when the isoprene peroxy radical reacts predominantly with NO, high NO_2/NO ratios lead to methacryloylperoxynitrate (MPAN) and SOA (*22*). MPAN reaction with the hydroxyl radical ($\cdot$OH) produces methacrylic acid epoxide (MAE) (*23*) as well as hydroxymethylmethyl-α-lactone (HMML) (*24*). MAE (*23*) and HMML (*24*) have been proposed as the isoprene SOA precursor under high-NO_x conditions, but the fate of HMML is somewhat uncertain given that similar analogues have short lifetimes (*25*). Both epoxides, IEPOX and MAE, can participate in acid-catalyzed ring-opening reactions in the particle phase (*26*), and higher isoprene aerosol concentrations have been linked with acidity ($[H^+]$) in laboratory experiments (*27*) and sulfate under ambient conditions (*7*).

In this paper, new aerosol-phase aqueous processes are incorporated into CMAQ to predict formation of key aerosol species from IEPOX (low-NO_x) and MPAN (high-NO_x). The parent

hydrocarbon distribution depends on NO_x, and the aqueous parameterization is a function of acidity as well as availability of aerosol-phase constituents including water and sulfate. Simulations for summer 2006 over the United States are compared to observations of individual species as well as to isoprene SOA modeled by Odum 2-product partitioning. Parameters with uncertainty are identified, and their effects on model predictions assessed. In addition, the model response to reductions in NO_x and SO_x emissions is examined.

Model Description

Chemical transport model

The Community Multiscale Air Quality (CMAQ) model (*28*) version 5.0.1 which treats advection, diffusion, gas-phase chemistry, aerosol processes, and deposition is used to simulate June 1 through August 31, 2006 conditions over the contiguous United States at 12 km by 12 km horizontal resolution with 35 vertical layers. Emissions are based on the 2005 National Emission Inventory (NEI) with year 2006 data for electric generating units and wildfires. Biogenic emissions are predicted inline with BEIS algorithms (*6*) using meteorology from WRF v3.3 processed by MCIP 4.0 (*29*). The CMAQ SAPRC07T chemistry (*30*) is expanded, adding over 150 new reactions and 34 new species, to include formation of IEPOX, MAE, and HMML in the gas phase (*23*, *31*) (Figure S1).

Aerosol-phase chemistry

CMAQ treats accumulation mode aerosol as an internal mixture of organic and inorganic constituents. Secondary inorganic aerosol, including ammonium and nitrate, is predicted using the thermodynamic equilibrium model ISORROPIA II (*32*). In this section, we define the base case model parameterization to include isoprene SOA from the Odum 2-product approach (*6*) in parallel to aerosol from isoprene epoxides with baseline parameters (Figure S1). Deviations from the base

case are described in the subsequent section entitled *Sensitivity simulations*.

Removal of existing model processes

The standard CMAQ treatment of isoprene SOA is based on an Odum 2-product fit for semivolatile aerosol using low-NO_x chamber experiments (*33*) followed by an acid enhancement under conditions of strong acidity and oligomerization of the particle phase to nonvolatile form using a fixed rate constant (*6*). In this work, the acid enhancement and oligomerization processes are removed since they are captured in a more mechanistic way by the new parameterization described below. The Odum 2-product semivolatile parameterization is retained as an estimate of semivolatile organic-phase isoprene aerosol production.

New processes added to the model

SOA formation from uptake of IEPOX and the sum of MAE and HMML onto aqueous aerosols is added to the model, while aerosol formation in cloud and fog droplets is neglected. For modeling purposes, HMML (57% yield from MPAN + ·OH) is treated like MAE (21 % yield from MPAN + ·OH) (*23*) in terms of heterogeneous uptake, providing an upper bound on the amount of SOA from MPAN.

The conversion of IEPOX and MAE + HMML to aerosol-phase species is accomplished via heterogeneous uptake onto accumulation mode aerosols. Uptake onto the aerosol phase can be parameterized using an uptake coefficient, γ, that can be calculated following (*34*):

$$\gamma = \left(\frac{1}{\alpha} + \frac{v}{4HRT\sqrt{D_a k_{particle}}} \frac{1}{f(q)} \right)^{-1} \tag{1}$$

$$f(q) = coth(q) - \frac{1}{q} \tag{2}$$

$$q = r_p \sqrt{\frac{k_{particle}}{D_a}} \tag{3}$$

where α is the mass accommodation coefficient (0.02 (*20*)), v is the mean molecular speed, H is

the Henry's Law coefficient, R is the gas constant, T is temperature, D_a is diffusivity in the aerosol phase (1×10^{-9} m^2 s^{-1} (*35*)), $k_{particle}$ is the pseudo first-order rate constant for reaction of the parent hydrocarbon in the aerosol phase, q is the diffuso-reactive parameter, and r_p is the effective particle radius. The Henry's Law coefficient for IEPOX and MAE are estimated to be 2.7×10^6 and 1.2×10^5 M atm^{-1} using HenryWin 3.2 (bond contribution method, (*36*)) (*37*). (See SI for additional details on model parameters and the implementation of uptake coefficients in CMAQ.)

The pseudo first-order particle-phase rate constant, $k_{particle}$, is calculated assuming protonation of the epoxide oxygen and nucleophilic addition. Eddingsaas et al. determined from information on isotopic effects and NMR analysis that epoxides similar to IEPOX follow an A-2 mechanism in which the rate determining step in the reaction is concerted nucleophilic addition to the ring (*26*). We assume the A-2 mechanism applies here; thus the particle-phase rate constant for an epoxide during a given model timestep (in which the concentrations of nucleophiles and acids are constant) is

$$k_{particle} = \sum_{i=1}^{N} \sum_{j=1}^{M} k_{i,j}[nuc_i][acid_j] \tag{4}$$

for N nucleophiles and M acids. Concentrations are expressed in molarity (mol L^{-1}). Seven new species are added to CMAQ to represent the results of particle phase reactions between nucleophiles and H^+ (a specific acid) or bisulfate (a general acid) (*26*) (Table 1). IEPOX (and MAE) form 2-methyltetrols (and 2-MG), organosulfates, and organonitrates as a result of addition of water, sulfate, and nitrate. These species can then serve as nucleophiles that add to an epoxide to form oligomers. Only dimers are currently considered (no higher-order oligomers) (*38*), and all dimers are lumped together. Currently, there is no precedent for including reactions of epoxides with other organic species in the particle phase and such additional pathways have not been considered.

Third-order rate constants for the particle-phase reactions ($k_{i,j}$) are based on the work of Eddingsaas et al. (*26*) and β-IEPOX, the proposed dominant IEPOX isomer mixture (*39*), when available (see Tables 1, S1, S2). Due to a lack of kinetic data, the MAE rate constants are assumed to be the same as for IEPOX. However, density functional calculations suggest that the barrier for the acid-catalyzed hydrolysis of MAE is higher than for IEPOX; thus, the rate constant may be

considerably smaller (*40*).

The concentrations of acids and nucleophiles in Eq. (4) are accumulation mode concentrations predicted by CMAQ using ISORROPIA II (*32*). Concentrations, usually expressed in μg m^{-3}, are converted to molarity using the entire accumulation mode volume (deviations from ideality are not treated in the kinetic calculations). The concentration of H^+ is based on the equilibrated Aitken and accumulation modes as calculated by ISORROPIA II. Since CMAQ transports only total sulfate in the particle, the ISORROPIA II predicted H^+ along with a charge balance are used to separate $SO_4{}^{2-}$ (nucleophile) and $HSO_4{}^-$ (general acid) for epoxide uptake.

Particle-phase reactions of IEPOX also lead to C_5-alkene triols (*22*) and *cis*- and *trans*-3-methyl-3,4-dihydroxytetrahydrofurans (*7*) which are not represented in the model. *Cis*- and *trans*-3-methyl-3,4-dihydroxytetrahydrofurans are significantly less abundant than the 2-methyltetrols (*7*, *41*). However, C_5-alkene triol concentrations can be significant (*7*, *41*). Since the C_5-alkene triols are not explicitly predicted by the model, the predictions of 2-methyltetrols may be overestimated. If the C_5-alkene triols also form from IEPOX in the presence of acid and water (hydrolysis), the modeled 2-methyltetrols might encompass both the 2-methyltetrols and C_5-alkene triols (*15*).

Sensitivity simulations

Sensitivity simulations are performed to examine the effects of changes in the model parameters and emissions. Two sensitivity simulations address uncertainty in the rates of particle-phase reaction and the Henry's Law coefficients (Eq. (1)). The rate constant for a given nucleophile with IEPOX should be related to the nucleophilic strength of that species (*42*). Although water is a weaker nucleophile than sulfate, rate constants in Table 1 indicate the opposite trend. Since the sulfate rate constant is based on experiments with nitrate and *cis*-2,3-epoxybutane-1,4-diol (Table S2), future work should better constrain the sulfate rate constant for IEPOX. To test the effect of the third-order $k_{i,j}$ rate constants on predictions of aerosol species, a sensitivity simulation is performed in which all the $k_{i,j}$ are set equal to the nitrate value (*sensitivity* $k_{i,j}$). This sensitivity simulation affects the relative tetrol to organosulfate split and thus the particle-phase speciation.

Chan et al. (*43*) estimated the Henry's Law coefficient of IEPOX to be 1.9×10^{7} M atm^{-1}, roughly a factor of seven higher than our baseline value. The second sensitivity simulation (*sensitivity H-law*, $k_{i,j}$) uses the nitrate-based rate constant from the first sensitivity simulation in addition to higher Henry's Law coefficients: the Chan et al. value for IEPOX (*43*) (1.9×10^{7} M atm^{-1}) and 1.2×10^{6} M atm^{-1} ($10\times$ higher than the baseline) for MAE. To a certain extent, this sensitivity simulation captures uncertainty in the Henry's Law coefficient as well as the overall particle-phase rate of reaction. It is expected to increase the overall magnitude of organic aerosol production while maintaining a speciation similar to *sensitivity* $k_{i,j}$. Changes to the estimated Henry's Law coefficient also affect wet scavenging but not dry deposition.

Two additional simulations examine the impact of reductions in emissions on isoprene SOA. Both emission control scenarios, a 25% reduction in anthropogenic and wildfire NO_x and a 25% reduction in all SO_x (SO_2 + $SO_4{}^{-2}$), are performed for July 2006 with the base model parameterization of heterogeneous uptake. All simulations contain traditional Odum 2-product semivolatile SOA in parallel to the new epoxide SOA (Figure S1).

Results and discussion

Model predictions

Base simulation

The new aerosol species are highest in concentration (Figure 1) where high rates of particle-phase reaction (Figure S3) coincide with significant isoprene emissions (Figure S2) allowing uptake of epoxides to the aerosol phase to compete with gas-phase ·OH reaction. The rate of particle-phase reaction is primarily governed by the rate of H^+ catalyzed ring-opening accompanied by addition of water producing 2-methyltetrols and 2-MG. The pseudo first-order particle-phase rate constants are highest (0.02 to 0.03 s^{-1}) where H^+ is also highest such as downwind of the Ohio River Valley during the modeled period (Figure S3(a)). This leads to significant isoprene aerosol over

West Virginia, but the highest isoprene aerosol concentrations tend to be over Alabama, where the concentration of IEPOX is higher.

Of the IEPOX-derived species, the hydrolysis products (2-methyltetrols) are predicted to dominate as a result of the relative abundance of aerosol water compared to other available nucleophiles. The organonitrates from IEPOX and MPAN are predicted to be the least abundant species due to low nitrate aerosol concentrations during the summer. A contribution to 2-methyltetrols and organosulfates from further reaction of organonitrates in the atmosphere (*44*) is not considered here because of the low concentrations of aerosol organonitrates in summer. The isoprene aerosol dimers (composed mostly of tetrol-tetrol dimers) are significantly less abundant than the monomers, while the IEPOX organosulfates and 2-MG are comparable in magnitude.

Aerosol from IEPOX generally exceeds the aerosol from MAE as a result of availability of gas-phase precursors (Figure S2) as well as the efficiency of uptake. Since IEPOX and MAE are treated the same in terms of particle-phase reaction rates, the difference in the uptake coefficients for MAE and IEPOX is entirely attributable to the difference in their Henry's Law coefficients. The IEPOX uptake coefficient predicted here is similar in magnitude to that of glyoxal (2.9×10^{-3} (*45*)) in locations of very high acidity, but lower elsewhere and generally below 10^{-3} across the Southeast. The factor of 20 lower Henry's Law coefficient for MAE compared to IEPOX leads to a similarly lower value of the uptake coefficient (1.4×10^{-4} or less) (Figure S3).

Vertical profiles

Models underestimate organic aerosol throughout the troposphere, and particularly for the lower 2km of the atmosphere in many pollution-influenced locations (*46*, *47*). Cloud-Aerosol Lidar with Orthogonal Polarization (CALIOP) instrument data further indicate that aerosol extinction is dominated by aerosols below 700 hPa (3 km) in the southeastern US (*48*). Model bias aloft has been shown to be a function of relative humidity, indicating a role for aqueous aerosol processing (*47*). The heterogeneous pathways implemented here lead to aerosol that is mostly confined to the lower 2 km of the atmosphere (Figure S5), similar to the aerosol of Couvidat et al. (*15*), and

different from the aqueous aerosol of Fu et al. (*49*) which peaked between 2 and 6 km. In addition, the new aerosol exceeds that from traditional semivolatile partitioning of isoprene products by more than 50% from 0.5 to 2.7 km, making it a candidate to close the measurement-model gap in the vertical distribution of organic aerosol. Note that the predicted vertical profile of MPAN-derived aerosol in this work indicates little support for higher 2-MG relative to IEPOX-derived aerosol despite MPAN reaction with ·OH increasing relative to thermal loss with altitude (Figure S5).

Uncertainty analysis

Across the eastern US, hydrolysis product (2-methyltetrol and 2-MG) and IEPOX-derived organosulfate concentrations vary significantly from the base case simulation due to changes in the third-order particle-phase reaction rate constants and Henry's Law coefficients (Figure 2). Decreasing the $k_{i,j}$ for nucleophilic addition of water (*sensitivity* $k_{i,j}$) decreases the hydrolysis products but leads to increases in the organosulfates as a result of less competition with water addition. Increasing the Henry's Law coefficients (*sensitivity H-law*, $k_{i,j}$) scales up the concentrations of aerosol species while roughly maintaining the relative ratios in *sensitivity* $k_{i,j}$. Note that organosulfates increase significantly in *sensitivity H-law*, $k_{i,j}$ which has both the lower rate constant for nucleophilic addition of water and higher Henry's Law coefficient.

Comparison to observations

Many of the new species, including 2-methyltetrols, 2-MG, and organosulfates, added to the model have been observed in the atmosphere, which allows for model evaluation. However, the spatial and temporal coverage of measurements is limited, which makes a quantitative evaluation across a large domain challenging. For individual species evaluation, we present the sensitivity simulations having the best agreement with observations (indicated in Figure 2 with diagonal lines).

Hydrolysis products

Daily integrated samples of 2-methylthreitol + 2-methylerythritol (both 2-methyltetrols) and 2-MG collected every sixth day during 2006 in Research Triangle Park (RTP), North Carolina (*50*) are paired in time and space with the model results. The base simulation for IEPOX tends to significantly overestimate 2-methyltetrols implying that tetrols may form less efficiently than our a priori parameters suggest or that IEPOX is overestimated. The lower rate constant for hydrolysis reactions (4.5$\times$ lower, *sensitivity* $k_{i,j}$) leads to the best agreement with 2-methyltetrol observations (depicted in Figure 3) but still overestimates 2-methyltetrol concentrations by 97 ng m^{-3} (107%) on average at RTP. Overestimates may arise from the absence of a competitive loss process of IEPOX to C_5-alkene triols. The base simulation (Figure 3, 2-MG), is able to capture 2-MG concentrations relatively well with only a -0.8 ng m^{-3} mean bias (-5% normalized mean bias).

Model predictions of semivolatile Odum 2-product isoprene SOA can be converted to estimates of 2-methyltetrols + 2-MG using composition information from laboratory experiments, providing a rough evaluation of traditional semivolatile SOA for comparison to the new pathways. Laboratory experiments report that 2-methyltetrols and 2-MG account for 6.3% of isoprene-derived SOA (*9*). Included in Figure 3 is the sum of hydrolysis products (2-methyltetrols and 2-MG) calculated using the laboratory speciation factor of 6.3% and Odum 2-product isoprene SOA. The concordance correlation coefficient (ccc) (*51*, *52*), a measure of both precision and accuracy, indicates that the new heterogeneous pathways (ccc=0.31 for 2-MG, ccc=0.28 for 2-methyltetrols) produce concentrations of isoprene aerosol constituents that are more consistent with observations than the traditional semivolatile absorptive partitioning pathway (ccc=0.07 for speciated Odum 2-product semivolatile isoprene SOA). The ccc for 2-methyltetrols from IEPOX could be further improved by additional decreases in the k_{water,H^+} rate constant below the *sensitivity* $k_{i,j}$ value. Using the rate constant for δ-IEPOX hydrolysis of 1.4$\times$10^{-4} M^{-2} s^{-1} for example (*53*), leads to a ccc of 0.39 and a mean bias of 49 ng m^{-3} (54% normalized mean bias).

Measurements of isoprene aerosol species from additional campaigns and time periods other than 2006 are compared to modeled June-July-August 2006 concentrations to understand whether

the new model captures spatial patterns (Figure 4 and abstract figure). Since the observations are not paired in time and campaigns may have targeted certain pollution events, the comparison should be viewed as illustrative, but the difference in concentrations between broad geographic regions such as California and the Southeast is expected to be relatively robust. Only model predictions from the simulations with best agreement (as determined by the RTP 2006 data) are shown. Most of the 2-methyltetrol comparisons fall within the factor of 2 range and indicate the model is capturing differences in locations such as California and the midwestern United States. Methylglyceric acid is not captured as well and modeled concentrations are more than a factor of 10 lower than observations for Bakersfield, California and Riverside, California (from 2010 and 2005 respectively). Gas-phase concentrations of MAE are predicted to exceed 100 ng m^{-3} in the model for Southern California (*23*) which would provide more than enough precursor to achieve the 2-MG concentrations observed, but minimal uptake to the aerosol phase occurs.

Organosulfates

Due to the limited duration of sampling campaigns, only a qualitative evaluation of the organosulfate concentrations predicted here is possible. The IEPOX organosulfate (molecular weight = 216 g mol^{-1}) has been detected at levels up to 515 ng m^{-3} (approximately 100 ng m^{-3} on average (*7*)) at the surface and 84 ng m^{-3} on average aloft in the troposphere (*54*). The MPAN organosulfate (2-MG sulfate ester) is less abundant in both the model results and observed concentrations for Yorkville, Georgia, where concentrations average 10 ng m^{-3} (*7*). Our model results suggest efficient formation of the IEPOX organosulfate at concentrations of 25 to 150 ng m^{-3} as a seasonal average in the southeastern United States with perhaps the best agreement with measurements from Yorkville, Georgia, in 2010 (*7*) for the most aggressive uptake ($sensitivity\ H\text{-}law, k_{i,j}$). The MPAN organosulfate concentrations from the base simulation are predicted to be less than 1 ng m^{-3} and could be significantly underestimated.

Total OC

Addition of aerosol from IEPOX and MPAN improves model performance of total OC in terms of magnitude and diurnal variation. Without the heterogeneous uptake pathways for IEPOX and MAE + HMML, CMAQ underestimates total OC by 1.15 μgC m^{-3} compared to the Chemical Speciation Network (CSN) and 0.29 μgC m^{-3} compared to the IMPROVE network during June-July-August 2006. The most aggressive uptake scenario examined (*sensitivity H-law*, $k_{i,j}$) is able to reduce that underestimate by 17% for CSN and 34% for IMPROVE. Observations from the Southeastern Aerosol Research and Characterization (SEARCH) study of OC indicate a relatively flat diurnal profile, while earlier versions of CMAQ (*6*) tend to have a pronounced nighttime high driven by primary organic aerosols and monoterpene + nitrate radical aerosol with additional influences from sesquiterpene SOA. The new isoprene SOA has a flatter diurnal profile with a slight daytime peak (Figure S6 and S7), which helps move the diurnal profile toward OC observations. Further supporting the heterogeneous uptake pathway as reasonable are the observed diurnal patterns of WSOC in Yorkville and Atlanta (*55*) and IEPOX-OA in Atlanta, Georgia, (*13*) which tend to be relatively flat or peak during the day. If the epoxide aerosol mechanism implemented in CMAQ is representative of IEPOX-OA (*13*) and can be scaled up to be consistent with the 33% contribution to total OA observed by Budisulistiorini et al. (*13*), it would effectively reduce the day/night imbalance in CMAQ in the Southeast.

Relative roles of IEPOX and MPAN aerosol

Observations (*7–10*, *43*, *50*, *56–58*) indicate that IEPOX-derived 2-methyltetrols generally dominate over MPAN-derived 2-MG, particularly during the summer. Exceptions to this trend include measurements taken downwind of Siberian biomass burning plumes (*59*), wintertime aerosol in the midwestern United States (*8*), and samples from Riverside and Bakersfield, California (*10*). In all exceptional cases, high-NO_x conditions as a result of proximity to NO_x emissions or higher NO to $HO_2\cdot$ ratios (as expected in winter, (*60*, *61*)) likely lead to enhanced 2-MG formation as a result of enhanced $RO_2\cdot$ + NO reactions. The model is generally consistent with data supporting

the dominance of 2-methyltetrols at the surface and aloft in the southeast United States.

The dominance of 2-methyltetrols over 2-MG can be explained by the pathways leading to their production and the relative amounts of their gas-phase precursors. Formation of IEPOX begins with isoprene reacting with ·OH followed by $HO_2\cdot$ to form hydroxyhydroperoxides (ISOPOOH). Further reaction of ISOPOOH with ·OH produces IEPOX in mass-based yields up to 61% under typical summertime conditions in the southeastern United States (*21*, *31*). Formation of MAE requires isoprene peroxyradicals to initially react with NO, decomposing to create methacrolein, followed by three more reactions forming MPAN and then MAE (*23*). Along the way, carbon is lost via competitive pathways that produce methylvinyl ketone and other species, thus, less than 5% of the initial isoprene forms MAE or HMML under typical southeastern U.S. conditions. Only when the rate of $RO_2\cdot$+NO exceeds $RO_2\cdot$+$HO_2\cdot$ by a factor of nine are the precursors to 2-MG expected to exceed IEPOX. These conditions could occur in NO_x source areas (e.g. urban areas) or during the winter. The higher Henry's Law coefficient for IEPOX compared to MAE also leads to higher 2-methyltetrol concentrations relative to 2-MG. If the acid-catalyzed ring-opening of MAE is slower than estimated here (*40*) as in *sensitivity* $k_{i,j}$, the model would likely underestimate 2-MG even more.

Implications of emission reductions for isoprene SOA

Effect of NO_x

Enhancements in biogenic SOA have been attributed to NO_x in the ambient atmosphere (*62*), but models examining the same effect (*63*, *64*) have not considered the dependence of SOA yield on peroxy radical fate as demonstrated here. For a 25% reduction in NO_x, semivolatile isoprene SOA is predicted to decrease (Figure 5), consistent with previous studies (*6*). In contrast, IEPOX-derived aerosol increases as the isoprene $RO_2\cdot$ fate is shifted away from the NO pathway and toward reaction with $HO_2\cdot$. This shift also leads to decreased MPAN-derived aerosol, but the change in the absolute magnitude of that aerosol is quite small in comparison to the IEPOX path (Figure S8). Since semivolatile aerosol production decreases while IEPOX-derived aerosol generally increases, the

relative role of these production pathways would determine the response of total isoprene aerosol (Figure S10(a)).

Inclusion of additional model processes could alter the response of isoprene SOA to reductions in NO_x. Aerosol from isoprene + $NO_3\cdot$ could contribute about one quarter of isoprene aerosol (*65*) and one third of all aerosol generated at night (*66*). Reductions in NO_x should lead to decreases in the NO_3 pathway thus at least partially offsetting the increase in IEPOX aerosol. However, this pathway is not yet represented in the model. The results presented here also do not capture formation of aerosol from glyoxal and methylglyoxal which should decrease under lower-NO_x conditions (*20*).

Effect of SO_x

Most sulfate and almost all SO_2 emitted in the United States is of anthropogenic origin (*64*, *67*). All of the epoxide aerosol, including the dominant isoprene aerosol species, 2-methyltetrols, depends on acidity and is thus subject to regulation by emissions of SO_x. A 25% reduction in SO_x is predicted to lead to a significant decrease in isoprene aerosol (Figure 5). The effect on semivolatile Odum 2-product isoprene aerosol is minor. However, both IEPOX- and MPAN-derived aerosol are significantly reduced as less acidity leads to slower rates of particle-phase reaction and less efficient uptake. Conversion of epoxides to the aerosol phase is further reduced by decreases in particle surface area. Changes in IEPOX-derived aerosol dominate the overall change in isoprene aerosol from all three pathways (Figure S9) resulting in predicted decreases up to 400-450 ng m^{-3} over the eastern United States. The decrease in isoprene SOA due to a reduction in SO_x is roughly a factor of 10 higher than the response due to a reduction in NO_x (Figure S10), making SO_x the likely anthropogenic control on epoxide-derived SOA in the eastern United States.

Future directions

While this new model framework makes considerable progress in addressing formation of specific isoprene aerosol constituents with significant ambient concentrations, a complete description of

isoprene aerosol, including glyoxal and methylglyoxal, and an expansion of processes examined here to the cloud phase is still needed to accurately capture how changes in anthropogenic emissions affect biogenic SOA. The sensitivity simulations employed here indicate a need to constrain the relative rates of particle-phase reactions leading to tetrols, organosulfates, and oligomers since organosulfates seem to form much more readily in the ambient than our a priori parameterization predicts (possibly due to an underestimated $k_{SO_4^{-2},H^+}$). And, although we have focused on the explicit production of seven isoprene aerosol species, isoprene can lead to additional aerosol in the atmosphere. Experiments connecting total IEPOX and MAE aerosol mass to the individual species would allow for improved attribution of ambient OC to isoprene. Ambient observations of classes or groups of compounds such as XRF sulfur-IC sulfate estimates of organosulfates (*68*) and AMS PMF factors (*12*, *13*) also need to be connected to these and other explicit estimates of specific isoprene SOA constituents.

Acknowledgement

The authors thank Prakash Bhave, Golam Sarwar, Wyat Appel, and Sergey Napelenok for useful discussion as well as SEARCH, CSN, and IMPROVE networks for data. The United States Environmental Protection Agency (EPA) through its Office of Research and Development funded and managed the research described here. This paper has been subjected to the Agency's administrative review and approved for publication. SLC was supported by an appointment to the Research Participation Program at the Office of Research and Development, US EPA, administered by ORISE. Y-HL and JDS were supported in part by the Electric Power Research Institute. Y-HL acknowledges a Dissertation Completion Fellowship from the UNC Graduate School.

Supporting Information Available

Additional equations, figures, and documentation are available. This material is available free of charge via the Internet at `http://pubs.acs.org/`.

References

(1) Zhang, Q. et al. Ubiquity and dominance of oxygenated species in organic aerosols in anthropogenically-influenced Northern Hemisphere midlatitudes. *Geophys. Res. Lett.* **2007**, *34*.

(2) Goldstein, A. H.; Koven, C. D.; Heald, C. L.; Fung, I. Y. Biogenic carbon and anthropogenic pollutants combine to form a cooling haze over the southeastern United States. *Proc. Nat. Acad. Sci. U.S.A.* **2009**, *106*, 8835–8840.

(3) Lewis, C. W.; Klouda, G. A.; Ellenson, W. D. Radiocarbon measurement of the biogenic contribution to summertime $PM_{2.5}$ ambient aerosol in Nashville, TN. *Atmos. Environ.* **2004**, *38*, 6053–6061.

(4) Glasius, M.; la Cour, A.; Lohse, C. Fossil and nonfossil carbon in fine particulate matter: A study of five European cities. *J. Geophys. Res.-Atmos.* **2011**, *116*.

(5) Guenther, A.; Karl, T.; Harley, P.; Wiedinmyer, C.; Palmer, P. I.; Geron, C. Estimates of global terrestrial isoprene emissions using MEGAN (Model of Emissions of Gases and Aerosols from Nature). *Atmos. Chem. Phys.* **2006**, *6*, 3181–3210.

(6) Carlton, A. G.; Bhave, P. V.; Napelenok, S. L.; Edney, E. D.; Sarwar, G.; Pinder, R. W.; Pouliot, G. A.; Houyoux, M. Model representation of secondary organic aerosol in CMAQv4.7. *Environ. Sci. Technol.* **2010**, *44*, 8553–8560.

(7) Lin, Y.-H.; Knipping, E. M.; Edgerton, E. S.; Shaw, S. L.; Surratt, J. D. Investigating the influences of SO_2 and NH_3 levels on isoprene-derived secondary organic aerosol formation using conditional sampling approaches. *Atmos. Chem. and Phys.* **2013**, in press.

(8) Lewandowski, M.; Jaoui, M.; Offenberg, J. H.; Kleindienst, T. E.; Edney, E. O.; Sheesley, R. J.; Schauer, J. J. Primary and secondary contributions to ambient PM in the midwestern United States. *Environ. Sci. Technol.* **2008**, *42*, 3303–3309.

(9) Kleindienst, T. E.; Jaoui, M.; Lewandowski, M.; Offenberg, J. H.; Lewis, C. W.; Bhave, P. V.; Edney, E. O. Estimates of the contributions of biogenic and anthropogenic hydrocarbons to secondary organic aerosol at a southeastern US location. *Atmos. Environ.* **2007**, *41*, 8288–8300.

(10) Lewandowski, M.; Piletic, I. R.; Kleindienst, T. E.; Offenberg, J. H.; Beaver, M. R.; Jaoui, M.; Docherty, K. S.; Edney, E. O. Secondary organic aerosol characterization at field sites across the United States during the spring-summer period. *Int. J. Environ. Anal. Chem.* **2013**, in press.

(11) Ding, X.; Zheng, M.; Yu, L.; Zhang, X.; Weber, R. J.; Yan, B.; Russell, A. G.; Edgerton, E. S.; Wang, X. Spatial and seasonal trends in biogenic secondary organic aerosol tracers and water-soluble organic carbon in the southeastern United States. *Environ. Sci. Technol.* **2008**, *42*, 5171–5176.

(12) Robinson, N. H. et al. Evidence for a significant proportion of secondary organic aerosol from isoprene above a maritime tropical forest. *Atmos. Chem. Phys.* **2011**, *11*, 1039–1050.

(13) Budisulistiorini, S. H.; Canagaratna, M. R.; Croteau, P. L.; Marth, W. J.; Baumann, K.; Edgerton, E. S.; Shaw, S. L.; Knipping, E.; Worsnop, D. R.; Jayne, J. T.; Gold, A.; Surratt, J. D. Real-time continuous characterization of secondary organic aerosol derived from isoprene epoxydiols (IEPOX) in downtown Atlanta, Georgia, using the Aerodyne Aerosol Chemical Speciation Monitor (ACSM). *Environ. Sci. Technol.* **2013**, *47*, 5686–5694.

(14) Lin, G.; Penner, J. E.; Sillman, S.; Taraborrelli, D.; Lelieveld, J. Global modeling of SOA formation from dicarbonyls, epoxides, organic nitrates and peroxides. *Atmos. Chem. Phys.* **2012**, *12*, 4743–4774.

(15) Couvidat, F.; Sartelet, K.; Seigneur, C. Investigating the impact of aqueous-phase chemistry and wet deposition on organic aerosol formation using a molecular surrogate modeling approach. *Environ. Sci. Technol.* **2012**, *47*, 914–922.

(16) Henze, D. K.; Seinfeld, J. H. Global secondary organic aerosol from isoprene oxidation. *Geophys. Res. Lett.* **2006**, *33*.

(17) Carlton, A. G.; Wiedinmyer, C.; Kroll, J. H. A review of secondary organic aerosol (SOA) formation from isoprene. *Atmos. Chem. Phys.* **2009**, *9*, 4987–5005.

(18) Zhang, X. L.; Liu, J. M.; Parker, E. T.; Hayes, P. L.; Jimenez, J. L.; de Gouw, J. A.; Flynn, J. H.; Grossberg, N.; Lefer, B. L.; Weber, R. J. On the gas-particle partitioning of soluble organic aerosol in two urban atmospheres with contrasting emissions: 1. Bulk water-soluble organic carbon. *J. Geophys. Res.-Atmos.* **2012**, *117*.

(19) Wozniak, A. S.; Bauer, J. E.; Dickhut, R. M. Characteristics of water-soluble organic carbon associated with aerosol particles in the eastern United States. *Atmos. Environ.* **2012**, *46*, 181–188.

(20) McNeill, V. F.; Woo, J. L.; Kim, D. D.; Schwier, A. N.; Wannell, N. J.; Sumner, A. J.; Barakat, J. M. Aqueous-phase secondary organic aerosol and organosulfate formation in atmospheric aerosols: A modeling study. *Environ. Sci. Technol.* **2012**, *46*, 8075–8081.

(21) Paulot, F.; Crounse, J. D.; Kjaergaard, H. G.; Kurten, A.; St Clair, J. M.; Seinfeld, J. H.; Wennberg, P. O. Unexpected epoxide formation in the gas-phase photooxidation of isoprene. *Science* **2009**, *325*, 730–733.

(22) Surratt, J. D.; Chan, A. W. H.; Eddingsaas, N. C.; Chan, M.; Loza, C. L.; Kwan, A. J.; Hersey, S. P.; Flagan, R. C.; Wennberg, P. O.; Seinfeld, J. H. Reactive intermediates revealed in secondary organic aerosol formation from isoprene. *Proc. Nat. Acad. Sci. U.S.A.* **2010**, *107*, 6640–6645.

(23) Lin, Y.-H. et al. Epoxide as a precursor to secondary organic aerosol formation from isoprene photooxidation in the presence of nitrogen oxides. *Proc. Nat. Acad. Sci. U.S.A.* **2013**, *110*, 6718–6723.

(24) Kjaergaard, H. G.; Knap, H. C.; Ornso, K. B.; Jorgensen, S.; Crounse, J. D.; Paulot, F.; Wennberg, P. O. Atmospheric Fate of Methacrolein. 2. Formation of Lactone and Implications for Organic Aerosol Production. *J. Phys. Chem. A* **2012**, *116*, 5763–5768.

(25) Chen, S.-Y.; Lee, Y.-P. Transient infrared absorption of t-CH3C(O)OO, c-CH3C(O)OO, and alpha-lactone recorded in gaseous reactions of CH3CO and O-2. *J. Chem. Phys.* **2010**, *132*.

(26) Eddingsaas, N. C.; VanderVelde, D. G.; Wennberg, P. O. Kinetics and products of the acid-catalyzed ring-opening of atmospherically relevant butyl epoxy alcohols. *J. Phys. Chem. A* **2010**, *114*, 8106–8113.

(27) Surratt, J. D.; Lewandowski, M.; Offenberg, J. H.; Jaoui, M.; Kleindienst, T. E.; Edney, E. O.; Seinfeld, J. H. Effect of acidity on secondary organic aerosol formation from isoprene. *Environ. Sci. Technol.* **2007**, *41*, 5363–5369.

(28) Foley, K. M.; Roselle, S. J.; Appel, K. W.; Bhave, P. V.; Pleim, J. E.; Otte, T. L.; Mathur, R.; Sarwar, G.; Young, J. O.; Gilliam, R. C.; Nolte, C. G.; Kelly, J. T.; Gilliland, A. B.; Bash, J. O. Incremental testing of the Community Multiscale Air Quality (CMAQ) modeling system version 4.7. *Geosci. Model Dev.* **2010**, *3*, 205–226.

(29) Otte, T. L.; Pleim, J. E. The Meteorology-Chemistry Interface Processor (MCIP) for the CMAQ modeling system: Updates through MCIPv3.4.1. *Geosci. Model Dev.* **2010**, *3*, 243–256.

(30) Hutzell, W. T.; Luecken, D. J.; Appel, K. W.; Carter, W. P. L. Interpreting predictions from the SAPRC07 mechanism based on regional and continental simulations. *Atmos. Environ.* **2012**, *46*, 417–429.

(31) Xie, Y.; Paulot, F.; Carter, W. P. L.; Nolte, C. G.; Luecken, D. J.; Hutzell, W. T.; Wennberg, P. O.; Cohen, R. C.; Pinder, R. W. Understanding the impact of recent advances in isoprene photooxidation on simulations of regional air quality. *Atmos. Chem. Phys. Discuss.* **2012**, 27173–27218.

(32) Fountoukis, C.; Nenes, A. ISORROPIA II: a computationally efficient thermodynamic equilibrium model for K^+-Ca^{2+}-Mg^{2+}-$NH_4{}^+$-Na^+-$SO_4{}^{2-}$-$NO_3{}^-$-Cl^--H_2O aerosols. *Atmos. Chem. Phys.* **2007**, *7*, 4639–4659.

(33) Kroll, J. H.; Ng, N. L.; Murphy, S. M.; Flagan, R. C.; Seinfeld, J. H. Secondary organic aerosol formation from isoprene photooxidation. *Environ. Sci. Technol.* **2006**, *40*, 1869–1877.

(34) Hanson, D. R.; Ravishankara, A. R.; Solomon, S. Heterogeneous reactions in sulfuric acid aerosols: A framework for model calculations. *J. Geophys. Res.* **1994**, *99*, 3615–3629.

(35) Gharagheizi, F.; Eslamimanesh, A.; Mohammadi, A. H.; Richon, D. Representation and prediction of molecular diffusivity of nonelectrolyte organic compounds in water at infinite dilution using the artificial neural network-group contribution method. *J. Chem. Eng. Data* **2011**, *56*, 1741–1750.

(36) Meylan, W. M.; Howard, P. H. Bond contribution method for estimating Henry's law constants. *Environ. Toxicol. Chem.* **1991**, *10*, 1283–1293.

(37) USEPA, Estimate Programs Interface Suite for Microsoft Windows, v4.11. 2012.

(38) Birdsall, A. W.; Zentener, C. A.; Elrod, M. J. Study of the kinetics and equilibria of the oligomerization reactions of 2-methylglyceric acid. *Atmos. Chem. Phys.* **2013**, *13*, 3097–3109.

(39) Paulot, F.; Crounse, J. D.; Kjaergaard, H. G.; Kroll, J. H.; Seinfeld, J. H.; Wennberg, P. O. Isoprene photooxidation: new insights into the production of acids and organic nitrates. *Atmos. Chem. Phys.* **2009**, *9*, 1479–1501.

(40) Piletic, I. R.; Edney, E. D.; Bartolotti, L. J. A computational study of acid catalyzed aerosol reactions of atmospherically relevant epoxides. **2013**, submitted.

(41) Lin, Y.-H.; Zhang, Z.; Docherty, K. S.; Zhang, H.; Budisulistiorini, S. H.; Rubitschun, C. L.; Shaw, S. L.; Knipping, E. M.; Edgerton, E. S.; Kleindienst, T. E.; Gold, A.; Surratt, J. D.

Isoprene epoxydiols as precursors to secondary organic aerosol formation: Acid-catalyzed reactive uptake studies with authentic compounds. *Environ. Sci. Technol.* **2012**, *46*, 250–258.

(42) Minerath, E. C.; Schultz, M. P.; Elrod, M. J. Kinetics of the reactions of isoprene-derived epoxides in model tropospheric aerosol solutions. *Environ. Sci. Technol.* **2009**, *43*, 8133–8139.

(43) Chan, M. N.; Surratt, J. D.; Claeys, M.; Edgerton, E. S.; Tanner, R. L.; Shaw, S. L.; Zheng, M.; Knipping, E. M.; Eddingsaas, N. C.; Wennberg, P. O.; Seinfeld, J. H. Characterization and quantification of isoprene-derived epoxydiols in ambient aerosol in the southeastern United States. *Environ. Sci. Technol.* **2010**, *44*, 4590–4596.

(44) Darer, A. I.; Cole-Filipiak, N. C.; O'Connor, A. E.; Elrod, M. J. Formation and stability of atmospherically relevant isoprene-derived organosulfates and organonitrates. *Environ. Sci. Technol.* **2011**, *45*, 1895–1902.

(45) Liggio, J.; Li, S.-M.; McLaren, R. Reactive uptake of glyoxal by particulate matter. *J. Geophys. Res.* **2005**, *110*, D10304.

(46) Volkamer, R.; Jimenez, J. L.; San Martini, F.; Dzepina, K.; Zhang, Q.; Salcedo, D.; Molina, L. T.; Worsnop, D. R.; Molina, M. J. Secondary organic aerosol formation from anthropogenic air pollution: Rapid and higher than expected. *Geophys. Res. Lett.* **2006**, *33*.

(47) Heald, C. L. et al. Exploring the vertical profile of atmospheric organic aerosol: Comparing 17 aircraft field campaigns with a global model. *Atmos. Chem. Phys.* **2011**, *11*, 12673–12696.

(48) Ford, B.; Heald, C. L. Aerosol loading in the southeastern United States: Reconciling surface and satellite observations. *Atmos. Chem. and Phys. Discuss.* **2013**, *13*, 9917–9952.

(49) Fu, T.-M.; Jacob, D. J.; Wittrock, F.; Burrows, J. P.; Vrekoussis, M.; Henze, D. K. Global budgets of atmospheric glyoxal and methylglyoxal, and implications for formation of secondary organic aerosols. *J. Geophys. Res.* **2008**, *113*, D15303.

(50) Offenberg, J. H.; Lewandowski, M.; Jaoui, M.; Kleindienst, T. E. Contributions of biogenic and anthropogenic hydrocarbons to secondary organic aerosol during 2006 in Research Triangle Park, NC. *Aerosol and Air Quality Research* **2011**, *11*, 99–108.

(51) Lin, L. I. A concordance correlation coefficient to evaluate reproducibility. *Biometrics* **1989**, *45*, 255–268.

(52) Lin, L. I. A note on the concordance correlation coefficient. *Biometrics* **2000**, *56*, 324–325.

(53) Cole-Filipiak, N. C.; O'Connor, A. E.; Elrod, M. J. Kinetics of the hydrolysis of atmospherically relevant isoprene-derived hydroxy epoxides. *Environ. Sci. Technol.* **2010**, *44*, 6718–6723.

(54) Froyd, K. D.; Murphy, S. M.; Murphy, D. M.; de Gouw, J. A.; Eddingsaas, N. C.; Wennberg, P. O. Contribution of isoprene-derived organosulfates to free tropospheric aerosol mass. *Proc. Nat. Acad. Sci. U.S.A.* **2010**, *107*, 21360–21365.

(55) Zhang, X.; Liu, Z.; Hecobian, A.; Zheng, M.; Frank, N. H.; Edgerton, S.; Weber, R. J. Spatial and seasonal variations of fine particle water-soluble organic carbon (WSOC) over the southeastern United States: implications for secondary organic aerosol formation. *Atmos. Chem. Phys.* **2012**, *12*, 6593–6607.

(56) Piletic, I. R.; Offenberg, J. H.; Olson, D. A.; Jaoui, M.; Krug, J.; Lewandowski, M.; Turlington, J. M.; Kleindienst, T. E. Constraining carbonaceous aerosol sources in a receptor model using combined 14C, redox species, organic tracers, and elemental/organic carbon measurements. **2013**, submitted.

(57) Kleindienst, T. E.; Lewandowski, M.; Offenberg, J. H.; Edney, E. O.; Jaoui, M.; Zheng, M.; Ding, X. A.; Edgerton, E. S. Contribution of primary and secondary sources to organic aerosol and $PM_{2.5}$ at SEARCH network sites. *Journal of the Air & Waste Management Association* **2010**, *60*, 1388–1399.

(58) Lewandowski, M.; Jaoui, M.; Kleindienst, T. E.; Offenberg, J. H.; Edney, E. O. Composition of $PM_{2.5}$ during the summer of 2003 in Research Triangle Park, North Carolina. *Atmos. Environ.* **2007**, *41*, 4073–4083.

(59) Ding, X.; Wang, X.; Xie, Z.; Zhang, Z.; Sun, L. Impacts of Siberian biomass burning on organic aerosols over the north Pacific Ocean and the Arctic: Primary and secondary organic tracers. *Environ. Sci. Technol.* **2013**, *47*, 3149–3157.

(60) Henze, D. K.; Seinfeld, J. H.; Ng, N. L.; Kroll, J. H.; Fu, T. M.; Jacob, D. J.; Heald, C. L. Global modeling of secondary organic aerosol formation from aromatic hydrocarbons: High- vs. low-yield pathways. *Atmos. Chem. Phys.* **2008**, *8*, 2405–2420.

(61) Ren, X. R. et al. Behavior of OH and HO_2 in the winter atmosphere in New York city. *Atmos. Environ.* **2006**, *40*, S252–S263.

(62) Shilling, J. E.; Zaveri, R. A.; Fast, J. D.; Kleinman, L.; Alexander, M. L.; Canagaratna, M. R.; Fortner, E.; Hubbe, J. M.; Jayne, J. T.; Sedlacek, A.; Setyan, A.; Springston, S.; Worsnop, D. R.; Zhang, Q. Enhanced SOA formation from mixed anthropogenic and biogenic emissions during the CARES campaign. *Atmos. Chem. Phys.* **2013**, *13*, 2091–2113.

(63) Lane, T. E.; Donahue, N. M.; Pandis, S. N. Effect of NO_x on secondary organic aerosol concentrations. *Environ. Sci. Technol.* **2008**, *42*, 6022–6027.

(64) Carlton, A. G.; Pinder, R. W.; Bhave, P. V.; Pouliot, G. A. To what extent can biogenic SOA be controlled? *Environ. Sci. Technol.* **2010**, *44*, 3376–3380.

(65) Pye, H. O. T.; Chan, A. W. H.; Barkley, M. P.; Seinfeld, J. H. Global modeling of organic aerosol: The importance of reactive nitrogen (NO_x and NO_3). *Atmos. Chem. Phys.* **2010**, *10*, 11261–11276.

(66) Rollins, A. W.; Browne, E. C.; Min, K. E.; Pusede, S. E.; Wooldridge, P. J.; Gentner, D. R.;

Goldstein, A. H.; Liu, S.; Day, D. A.; Russell, L. M.; Cohen, R. C. Evidence for NO_x control over nighttime SOA formation. *Science* **2012**, *337*, 1210–1212.

(67) Bates, T. S.; Lamb, B. K.; Guenther, A.; Dignon, J.; Stoiber, R. E. Sulfur emissions to the atmosphere from natural sources. *Journal of Atmospheric Chemistry* **1992**, *14*, 315–337.

(68) Tolocka, M. P.; Turpin, B. Contribution of organosulfur compounds to organic aerosol mass. *Environ. Sci. Technol.* **2012**, *46*, 7978–7983.

Table 1: New isoprene SOA species considered in the CMAQ model along with their molecular weight, OM/OC ratio, parent hydrocarbon identity, nucleophile that adds to the parent, and rate constants for H^+ and $HSO_4{}^-$ catalyzed ring-opening reactions (*26*). OS denotes organosulfate while ON denotes organonitrate. See Table S1 and S2 for additional information.

Species	MW [g mol^{-1}]	$\frac{OM}{OC}$	Parent Hydrocarbon	Nucleophile Added	k_{i,H^+} [M^{-2}s^{-1}]	k_{i,HSO_4^-} [M^{-2}s^{-1}]
2-methyltetrol	136	2.27	IEPOX	water	9.0×10^{-4} [a]	1.3×10^{-5}
IEPOX-derived OS	216	3.60	IEPOX	sulfate	2.0×10^{-4} [b]	2.9×10^{-6}
IEPOX-derived ON	181	3.02	IEPOX	nitrate	2.0×10^{-4}	2.9×10^{-6}
2-MG	120	2.50	MAE, HMML	water	9.0×10^{-4}	1.3×10^{-5}
MPAN-derived OS	200	4.17	MAE, HMML	sulfate	2.0×10^{-4} [b]	2.9×10^{-6}
MPAN-derived ON	165	3.44	MAE, HMML	nitrate	2.0×10^{-4}	2.9×10^{-6}
dimers (as tetrol dimer)	248	2.07	IEPOX	2-methyltetrol	2.0×10^{-4}	2.9×10^{-6}
			IEPOX	IEPOX-derived OS	2.0×10^{-4}	2.9×10^{-6}
			IEPOX	IEPOX-derived ON	2.0×10^{-4}	2.9×10^{-6}
			MAE, HMML	2-MG	2.0×10^{-4}	2.9×10^{-6}
			MAE, HMML	MPAN-derived OS	2.0×10^{-4}	2.9×10^{-6}
			MAE, HMML	MPAN-derived ON	2.0×10^{-4}	2.9×10^{-6}

[a] Sensitivity analysis indicates this value is too high and a value of 2.0×10^{-4} M^{-2}s^{-1} is more consistent with observations of 2-methyltetrols.

[b] Sensitivity analysis indicates this value might be too low and that additional investigation is needed.

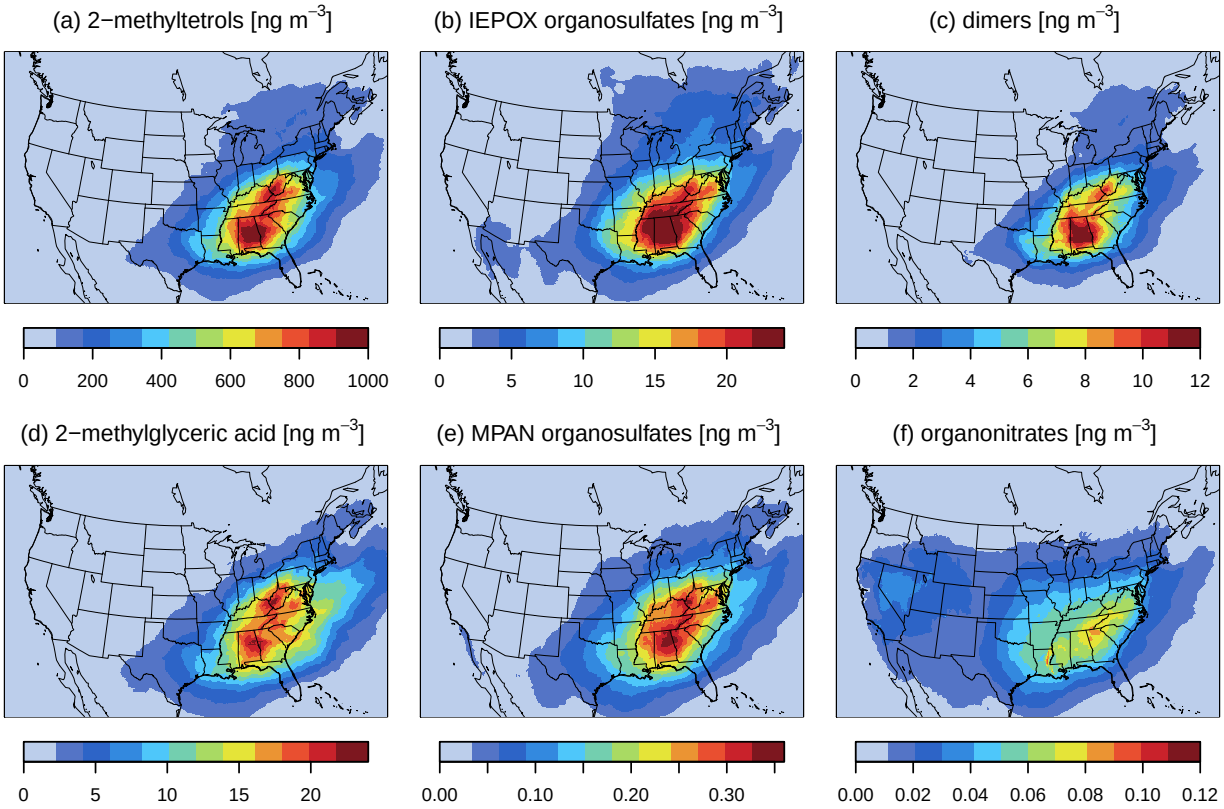

Figure 1: Predicted mean concentrations for July-July-August 2006 of (a) 2-methyltetrols, (b) IEPOX-derived organosulfates, (c) isoprene aerosol dimers, (d) 2-MG, (e) MPAN-derived organosulfates, and (f) IEPOX- and MPAN-derived organonitrates for the base simulation.

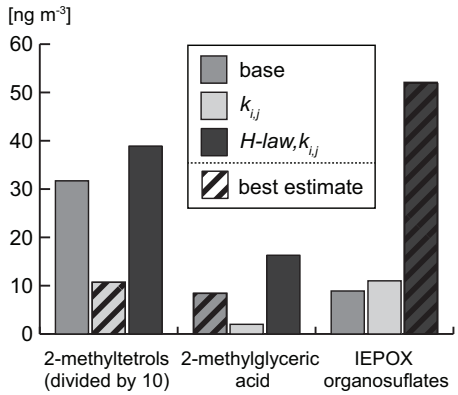

Figure 2: Effect of sensitivity simulations on three major isoprene-derived aerosol-phase consituents for June-July-August 2006. *Sensitivity* $k_{i,j}$ reduces the rate constant for nucleophilic addition of water to the value used for nitrate (2×10^{-4} M atm^{-1}, Table 1). *Sensitivity H-law*, $k_{i,j}$ uses the same particle-phase rate constants as *sensitivity* $k_{i,j}$, but increases the Henry's law coefficients by a factor of 7 and 10 for IEPOX and MAE, respectively. Concentrations are averaged over a 2,412 km by 2,052 km portion of the eastern United States. Predictions with the best agreement with observations are indicated with diagonal lines.

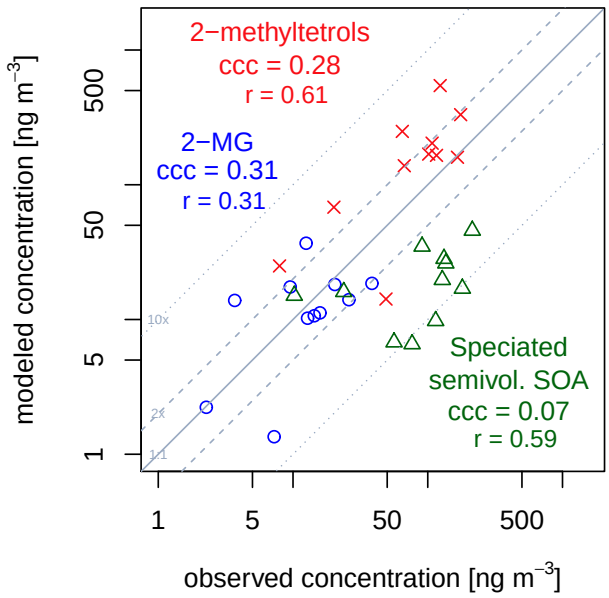

Figure 3: Observed (*50*) and predicted concentrations of 2-methyltetrols (red x) and 2-MG (blue circle) in Research Triangle Park, North Carolina during 2006. Also shown is the calculated sum 2-methyltetrols and 2-MG (green triangle) based on speciating semivolatile isoprene SOA with a laboratory based factor. The concordance correlation coefficient (ccc) and Pearson r are shown for each set of model-observation pairs. Model results are only shown for the sensitivity simulations indicated by diagonal lines in Figure 2.

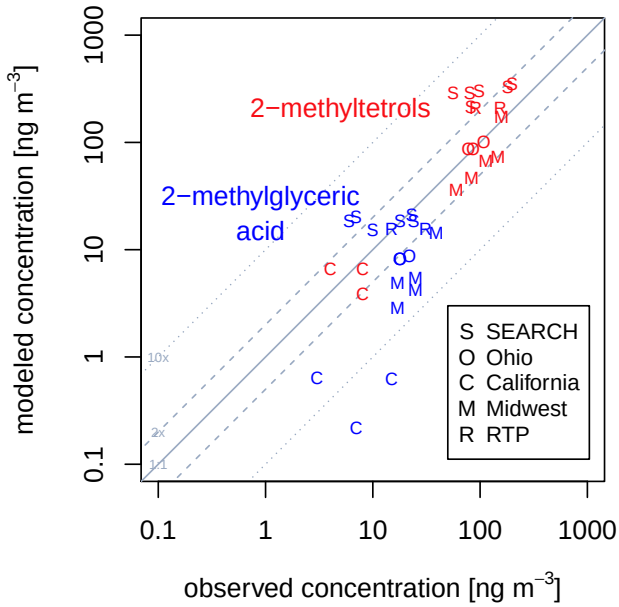

Figure 4: Observed and modeled concentrations of isoprene aerosol species across the United States. Observations include measurements from SEARCH sites in 2005 (*57*) and 2008 (*43*) (S), the Cleveland Multiple Air Pollutant Study in Ohio during 2009 (O) (*10*, *56*), Pasadena and Bakersfield (California Research at the Nexus of Air Quality and Climage Change, CalNex, 2010) and Riverside (Study of Organic Aerosols in Riverside, SOAR, 2005) in California (C) (*10*), the Midwest Urban Organics Study in 2004 (M) (*8*), and Research Triangle Park in North Carolina during 2003 (*58*) and 2006 (*50*) (R). Observations are limited to May through September and compared to a model June-July-August 2006 average for each location. Model results are only shown for the sensitivity simulations indicated by diagonal lines in Figure 2. The information is also presented graphically in the abstract.

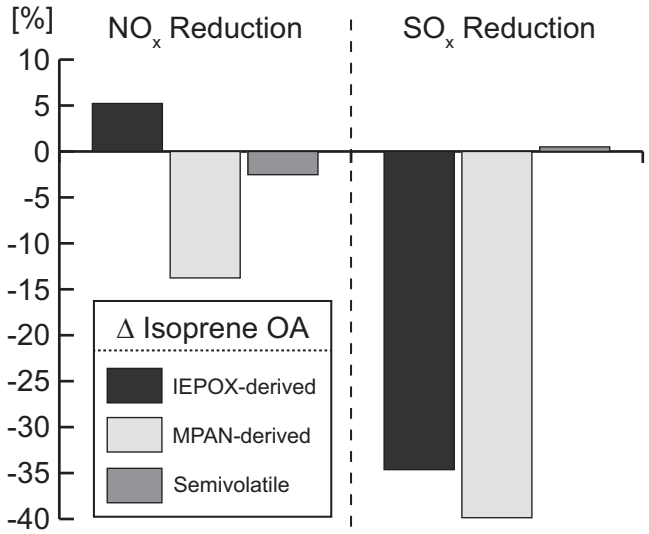

Figure 5: Predicted percent change in IEPOX-derived, MPAN-derived, and semivolatile (Odum 2-product) isoprene SOA over the eastern United States for a 25% reduction in anthropogenic and wildfire-derived NO_x and a 25% reduction in SO_x relative to a base simulation for July 2006. The effect on isoprene dimers (a minor species) is not shown.

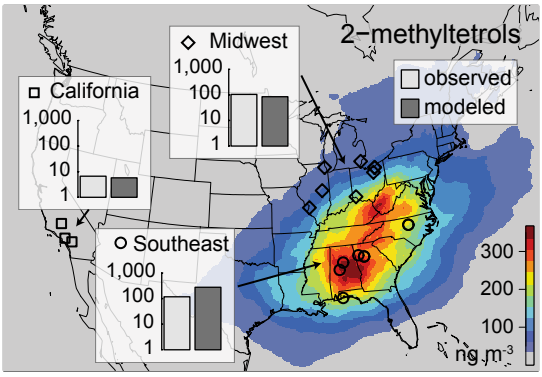
2−methyltetrols
observed
modeled
Midwest
California
Southeast
1,000
100
10
1
300
200
100
ng m-3

Supporting Information for:

Epoxide pathways improve model predictions of isoprene markers and reveal key role of acidity in aerosol formation

Havala O. T. Pye, Robert W. Pinder, Ivan R. Piletic, Ying Xie, Shannon L. Capps, Ying-Hsuan Lin, Jason D. Surratt, Zhenfa Zhang, Avram Gold, Deborah J. Luecken, William T. Hutzell, Mohammed Jaoui, John H. Offenberg, Tadeusz E. Kleindienst, Michael Lewandowski, and Edward O. Edney

US Environmental Protection Agency, National Exposure Research Laboratory, Research Triangle Park, North Carolina, USA; Shanghai Meteorological Service, Shanghai, China; University of North Carolina at Chapel Hill, Department of Environmental Science and Engineering, Chapel Hill, North Carolina, USA; and Alion Science and Technology, Box 12313, Research Triangle Park, North Carolina, USA

E-mail: Pye.havala@epa.gov

This supporting information contains 15 pages: 2 tables, 10 figures.

Additional Model Documentation

Equations

In CMAQ, the calculated value of γ (Eq. 1, main manuscript) is used to convert gas-phase IEPOX and MAE+HMML to aerosol-phase species. The change in gas-phase precursor during a model timestep of length Δt is computed using[1]:

$$\Delta precursor = precursor_i \left[\exp\left(-\frac{A}{\frac{r_p}{D_g} + \frac{4}{\nu_i \gamma_i}} \Delta t \right) - 1] \right] \quad \text{(S1)}$$

where $\Delta precursor$ is the change in IEPOX, MAE, or HMML, $precursor_i$ is the initial species concentration at the beginning of the model timestep, A is the aerosol surface area, r_p is the effective particle radius, D_g is the diffusivity in the gas phase (10^{-5} m s^{-1} at standard conditions), ν_i is the mean molecular speed, and γ_i is calculated following Eq. 1 for IEPOX and MAE. The mean molecular speed is calculated following[2]:

$$\nu_i = \sqrt{\frac{8RT}{\pi M_i}} \quad \text{(S2)}$$

where R is the universal gas constant, T is temperature, and M_i is the molecular weight of species i. The amount of precursor removed from the gas phase according to Eq. S1 is converted to the aerosol phase with appropriate increases in mass due to addition of oxygen, sulfate, etc. The aerosol is speciated according to the relative rates of particle-phase reaction.

Particle-phase rate constants

Tables S1 and S2 provide more detail on the particle-phase reaction rate constants used in Eq. (4) of the main manuscript. Experimental and modeling work indicates that the rate constant for hydrolysis of IEPOX ranges from 0.0079 to 0.05 M^{-1} s^{-1} with 3-methyl-3,4-epoxy-1,2 butane diol (δ-IEPOX) having lower values than 2-methyl-2,3-epoxy-1,4 butanediol (β-IEPOX) (see Table S1). Given that β-IEPOX likely accounts for ~70% of IEPOX[3], we use 0.05 M^{-1} s^{-1} as our baseline value. For the hydrolysis reaction, the concentration of the nucleophile, water, was not varied and a second-order rate constant was estimated by Eddingsaas et al.[4] For an A-2 mechanism (as is assumed for IEPOX and MAE based on Eddingsaas et al.), the water concentration is effectively incorporated into the rate constant. The pseudo second-order hydrolysis rate constant for β-IEPOX from Eddingsaas et al. is converted to a third-order rate constant by dividing by the molarity of water (55 mol L^{-1}), thus allowing the model parameterization to account for the concentration of aerosol water in the rate of particle-phase epoxide reaction (Table S2). The ratio of the water to the other nucleophile $k_{i,j}$ constants is assumed to be the same whether H^+ or HSO_4^- acts as the acid. Sulfate rate constants are assumed equal to the nitrate value[4-5] and also applied to the monomers (Table S2).

Table S1: Estimates of second-order IEPOX hydrolysis rate constants in currently available studies.

Species	Eddingsaas et al.[4] estimate based on structure k [M^{-1} s^{-1}]	Cole-Filipiak et al.[6] experiment k [M^{-1} s^{-1}]	Cole-Filipiak et al.[6] model k [M^{-1} s^{-1}]
cis- + *trans*-2-methyl-2,3-epoxy-1,4-butanediol (β-IEPOX)[1]	0.05	0.036	0.052
3-methyl-3,4-epoxy-1,2-butanediol (δ-IEPOX)	0.05	0.0079	0.013

[1] Paulot et al.[3] estimate ~70% of the isoprene peroxy radical is β in form.

Table S2: Conversion of IEPOX acid-catalyzed ring-opening rate constants in the work of Eddingsaas et al. to model ready values (final numbers are summarized in Table 1).

Rate Constant	Eddingsaas et al.[4] value	Model-ready value [M^{-2} s^{1}]	Notes
k_{water,H^+}	0.05 M^{-1} s^{-1}	0.05/55.55=9.0 x 10^{-4}	Based on *cis*- + *trans*-2-methyl-2,3-epoxy-1,4-butanediol (β-IEPOX). See Table S1 for more information. Removed concentration of water (55.5 mol L^{-1}).
$k_{sulfate,H^+}$	2±1 x 10^{-4} M^{-2} s^{1}	2 x 10^{-4}	Same as nitrate as recommended by Eddingsaas et al.
$k_{nitrate,H^+}$	2±1 x 10^{-4} M^{-2} s^{1}	2 x 10^{-4}	Experimentally determined for cis-2,3-epoxybutane-1,4-diol in a $HNO_3/NaNO_3$ solution
$k_{monomer,H^+}$	NA[1]	2 x 10^{-4}	Assumed equal to nitrate value.
$k_{water,HSO4^-}$	7.3±0.3 x 10^{-4} M^{-1} s^{1}	7.3 x 10^{-4} /55.55= 1.31 x 10^{-5}	Determined for *cis*-2,3-epoxybutane-1,4-diol in a H_2SO_4/Na_2SO_4 solution using the previously determined rate constants for H^+ catalyzed addition of sulfate and water. Removed concentration of water (55.5 mol L^{-1}).
$k_{sulfate,HSO4^-}$	NA	1.31 x 10^{-5}*2/9= 2.9 x 10^{-6}	Scaled $k_{water,HSO4^-}$ using the ratio of k_{nuc,H^+} to k_{water,H^+} where nuc is any nucleophile other than water
$k_{nitrate,HSO4^-}$	NA	1.31 x 10^{-5}*2/9= 2.9 x 10^{-6}	
$k_{monomer,HSO4^-}$	NA	1.31 x 10^{-5}*2/9= 2.9 x 10^{-6}	

[1]Not applicable

Sensitivity to parameters

In the main manuscript, the sensitivity of model predictions to values of the particle-phase rate constants ($k_{i,j}$) and Henry's law coefficients were tested. The model is not expected to be sensitive to the values of α, D_a, or D_g unless they are poorly estimated (by a factor of ~100).

The uptake coefficient, γ, should approach the value of the accommodation coefficient, α, at very high rates of particle-phase reaction. Figure S3 (d-e), indicates that the uptake coefficient is generally a factor of 10 or more smaller than the accommodation coefficient of 0.02 and is not approaching that value. Since the base simulation overpredicts methyltetrols, the γ in Figure S3 (d) is also likely over predicted. Thus, the accommodation coefficient would need to be significantly (more than a factor of 10, likely more than a factor of 100) smaller than the 0.02 value to limit uptake and influence predictions.

The particle phase reaction is sufficiently slow ($k_{particle} < 1\ s^{-1}$) such that the diffuso-reactive parameter (Eq. 2) is significantly less than the value of one for an accumulation mode particle (200 nm diameter). As a result[1], $f(q) \approx q/3$, and the aerosol-phase diffusivity (D_a) effectively cancels out of Eq. 1. We expect the predicted uptake coefficients to be valid for $D_a \geq 10^{-15}\ m^2\ s^{-1}$. The lower bound of this range ($10^{-15}\ m^2\ s^{-1}$) falls within the range of diffusivities estimated for organics in α-pinene SOA when the relative humidity is above 40%[7].

The gas-phase diffusivity will be important if the uptake coefficient or particle size is very large. For accumulation mode particles (200 nm diameter) with $\gamma < 0.02$, the model is not sensitive to D_g since the term with γ dominates over r_p/D_g in equation S1.

Additional Figures

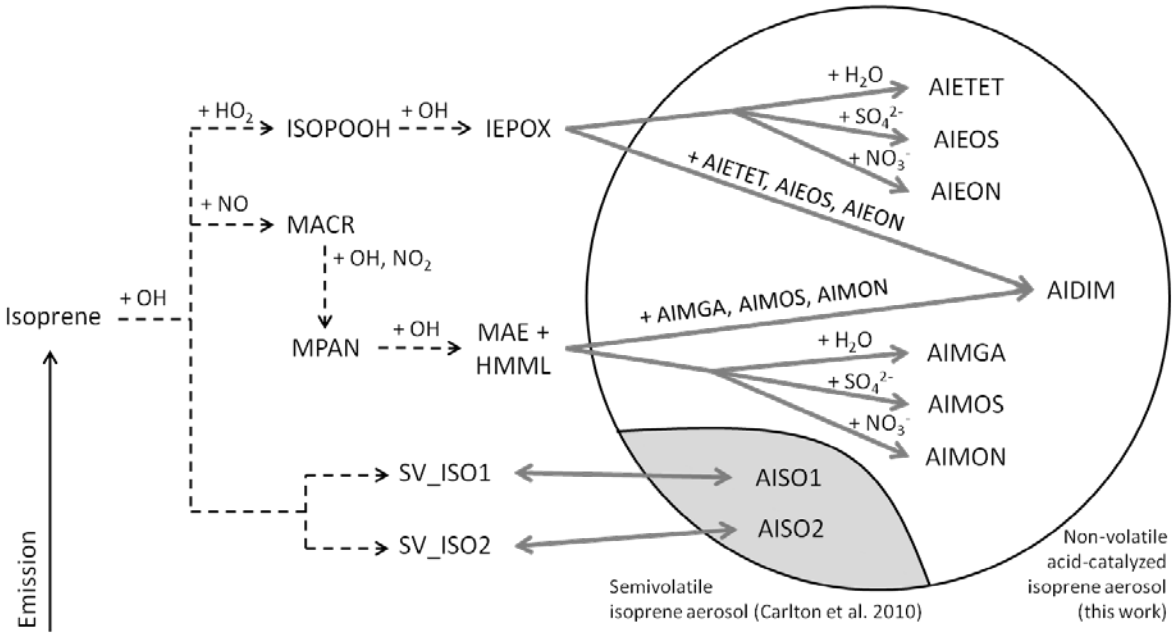

Figure S1: Schematic of updated isoprene aerosol treatment in CMAQ. Dashed lines summarize gas-phase chemistry leading to IEPOX[8], MAE+HMML[9], and semivolatile Odum 2-product isoprene SOA[10]. Expansion of the SAPRC07TC chemical mechanism in CMAQ[11] to include the explicit formation of IEPOX, MAE, and HMML in the gas phase has been previously described[8-9] and is briefly summarized here. The SAPRC07TC mechanism includes reactions of isoprene with OH, NO_3 and O_3, but epoxides form only through the OH reaction. The discrimination between the epoxides depends on the fate of the initial isoprene peroxy radical that is formed after H-abstraction by OH, as shown above. Under lower-NO_x conditions, when the peroxy radical reacts with HO_2, IEPOX is formed relatively promptly. In contrast, under high-NO_x conditions, when the radical reacts with NO, a series of alternate reactions is simulated, with methacrolein as one of the products. Under favorable conditions (high NO_2/NO ratios), the methacrolein can form MPAN which can further react to produce both MAE and HMML. While the IEPOX in the lower-NO_x pathway can be formed after three reactions, MAE and HMML formation in the high-NO_x route requires a minimum of 5 reactions, with many competing reactions forming other products, thus decreasing the yield of SOA precursors.

In the particle phase, IEPOX is shown reacting with water, sulfate, and nitrate leading to 2-methyltetrols (AIETET), organosulfates (AIEOS), and organonitrates (AIEON). Similarly, MAE+HMML form 2-methylglyceric acid (AIMGA), organosulfates (AIMOS), and organonitrates (AIMON). Oligomers in the form of dimers (AIDIM) result when the epoxides react with one of the existing epoxide-derived aerosol species. All of the epoxide reactions are modeled as acid-catalyzed reactions. Properties of each new aerosol compound, including molecular weights, are shown in Table 1 of the main manuscript.

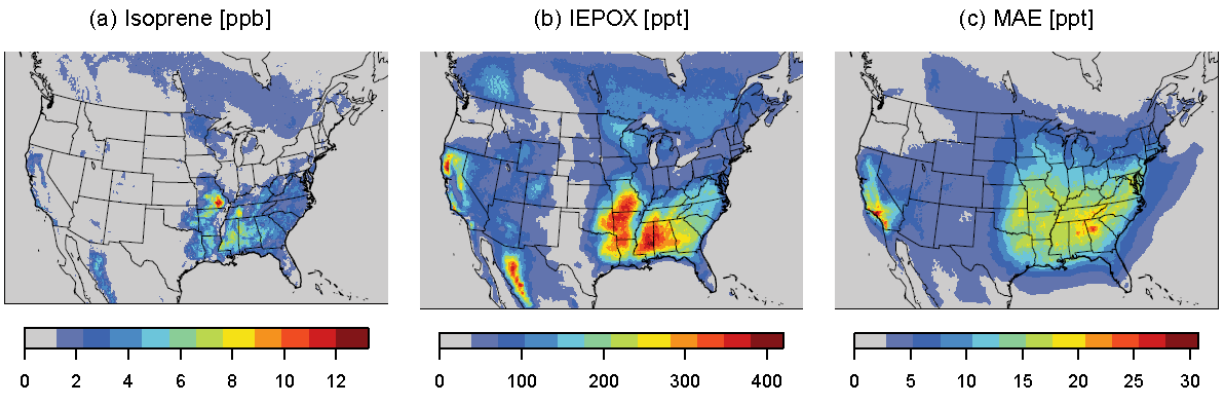

Figure S2: Gas-phase species leading to aerosol: isoprene, IEPOX, and MAE. Concentrations are from a base simulation averaged for June-July-August 2006.

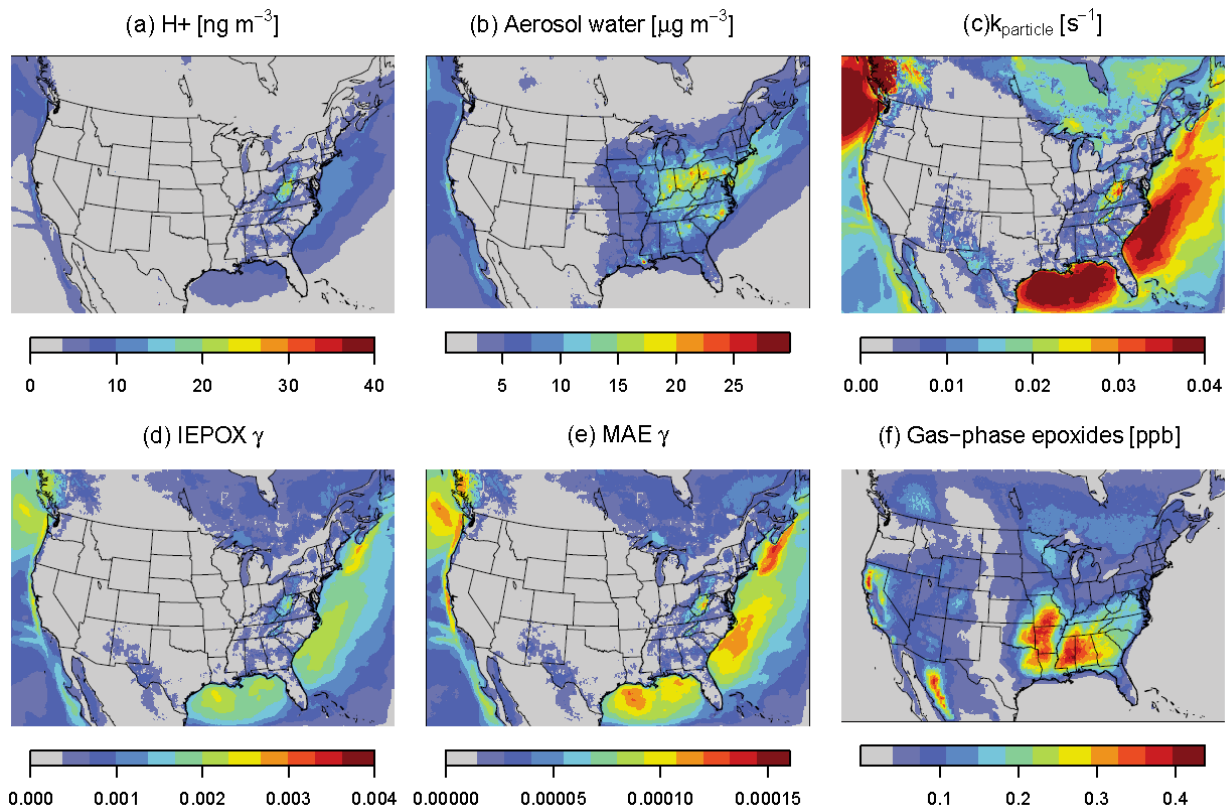

Figure S3: (a) Particle-phase H+ (based on ISORROPIA II[12]), (b) accumulation mode aerosol water (based on ISORROPIA II[12]), (c) first order rate constant for IEPOX reaction in the particle phase, (d) uptake coefficient for IEPOX, (e) uptake coefficient for MAE, and (f) gas-phase IEPOX + MAE available for uptake as predicted by CMAQ for June-July-August 2006 in the base simulation.

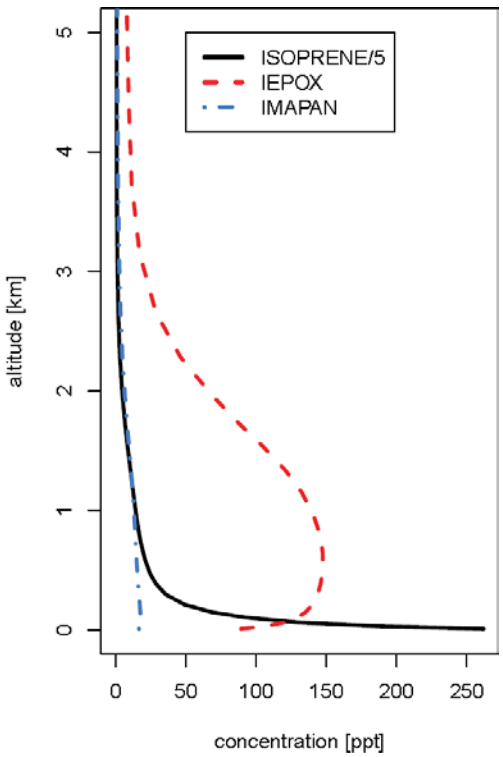

Figure S4: Vertical profile of predicted isoprene (divided by 5), IEPOX, and isoprene-derived MPAN averaged over the eastern United States for June 19-25, 2006 in a base simulation.

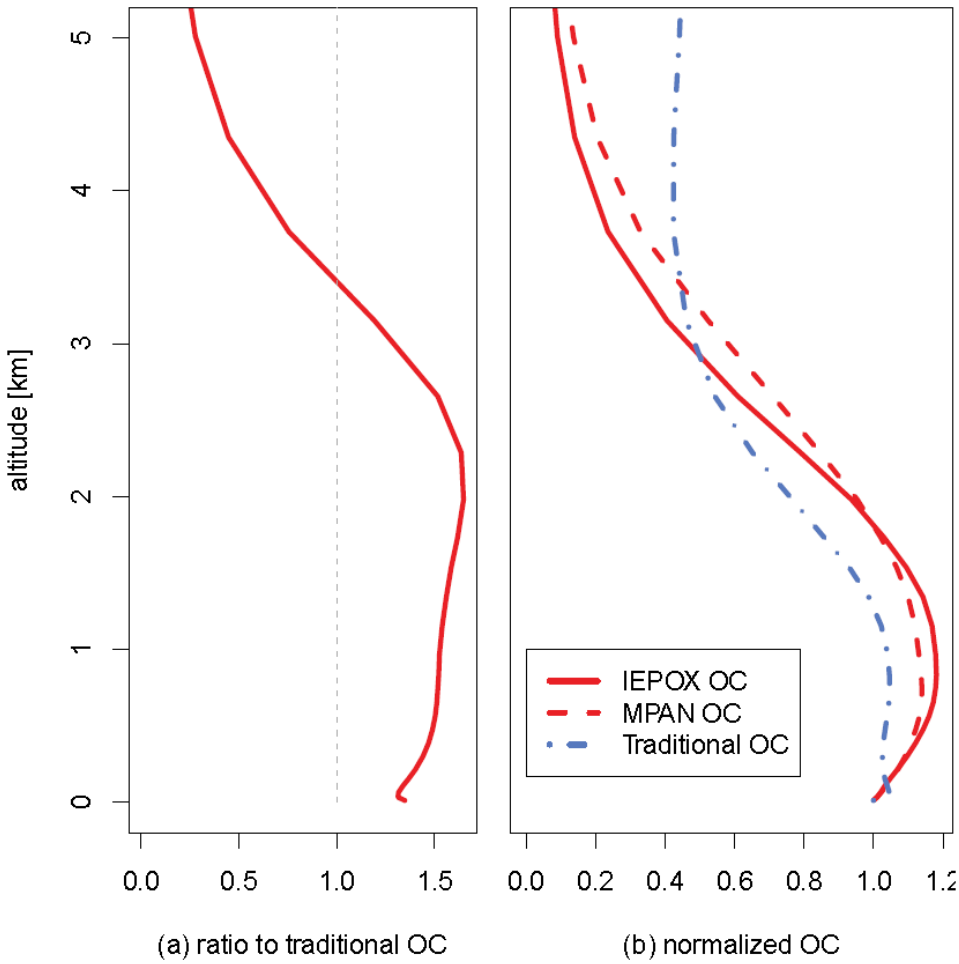

Figure S5: (a) Ratio of IEPOX and MPAN-derived OC to traditional semivolatile isoprene OC. (b) Vertical profile of IEPOX (2-methyltetrols, organosulfates, organonitrates), MPAN (methylglyceric acid, organosulfates, organonitrates), and traditional isoprene OC normalized to layer 1. Both panels are averaged over the eastern United States for June 19-25, 2006 in a base simulation.

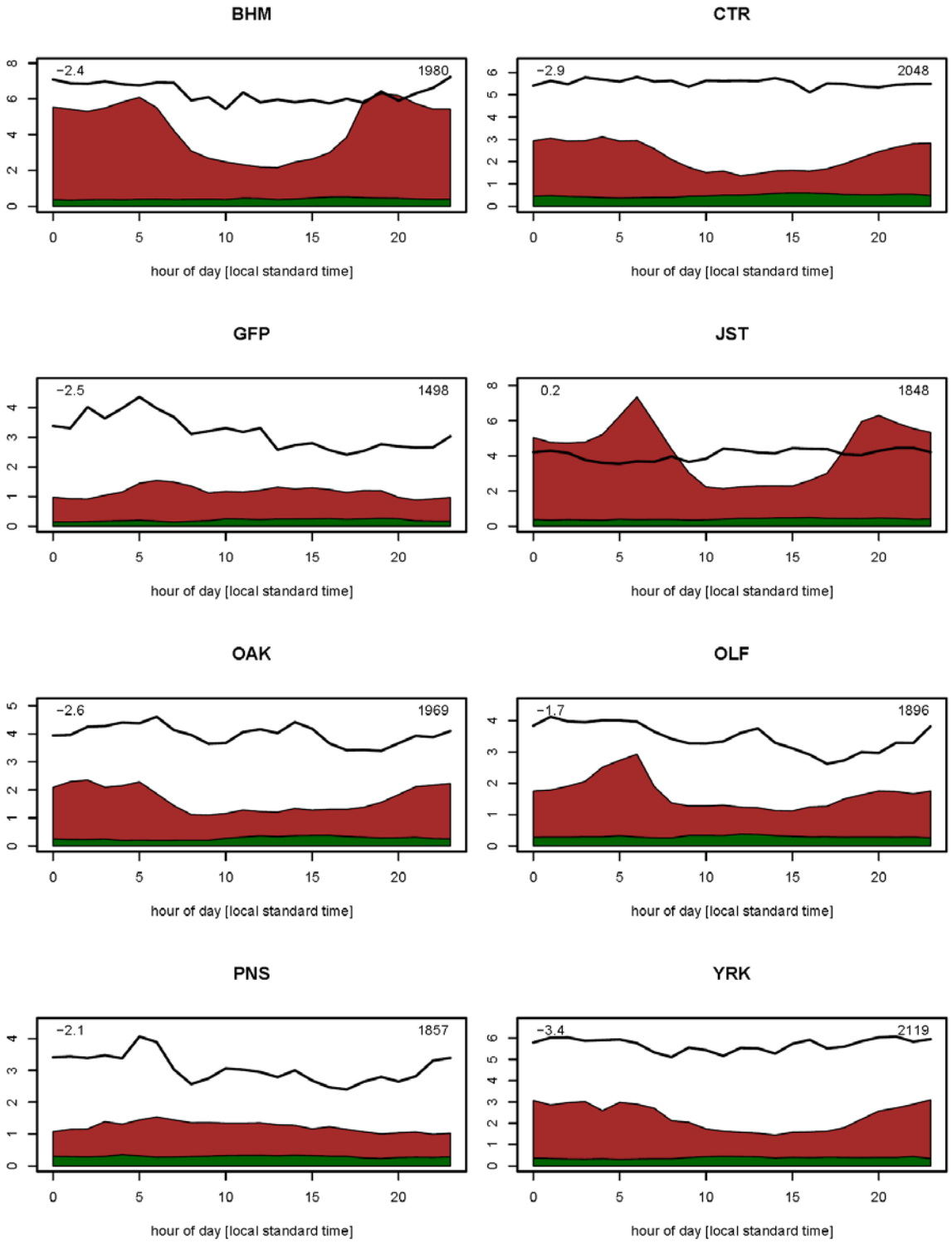

Figure S6: Observed (black line) and predicted (filled curve, *sensitivity H-law*,$k_{i,j}$) hourly OC at SEARCH sites during June-July-August 2006. The mean bias (in μgC/m^3) (upper left) along with the number of observations (upper right) is shown for each site. The brown portion represents total model OC (from all sources including isoprene) while the green portion represents only isoprene SOA from heterogeneous reactions of IEPOX and MPAN.

Centreville, AL

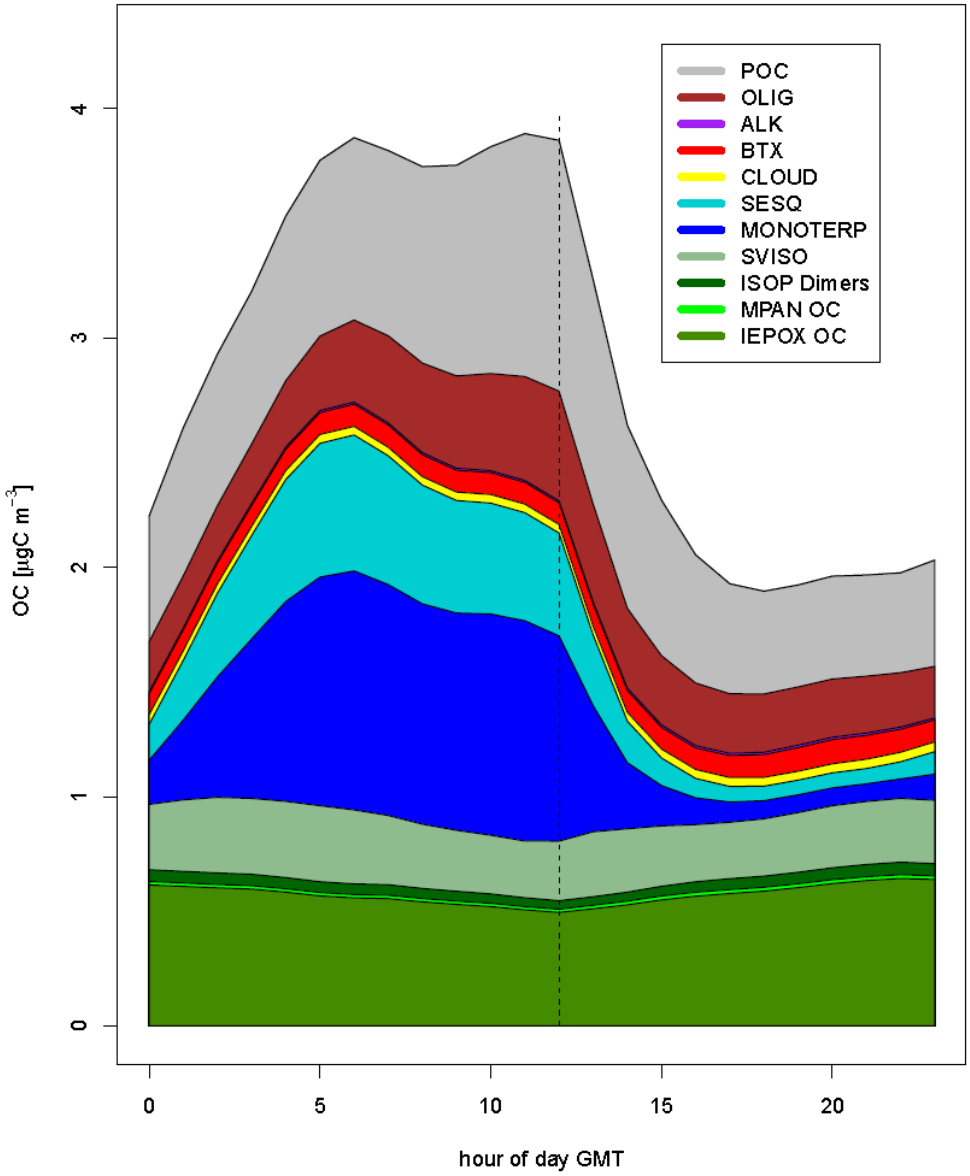

Figure S7: Composition of OC in Centreville, AL (SEARCH location CTR) as predicted by CMAQ (*sensitivity H-law*,$k_{i,j}$) June – August 2006 from sensitivity 2. Aerosol includes primary organic carbon (POC), oligomers (OLIG), alkane SOA (ALK), single-ring aromatic SOA (BTX), SOA produced in cloud from glyoxal and methylglyoxal (CLOUD), sesquiterpene SOA (SESQ), monoterpene SOA (MONOTERP), semivolatile isoprene SOA as predicted by the Odum 2-product model (SVISO), dimers produced from heterogeneous epoxide reactions (ISOP Dimers), MPAN-derived OC (MPAN OC), and IEPOX-derived OC (IEPOX OC). The vertical dashed line marks 6am CST (7am EST).

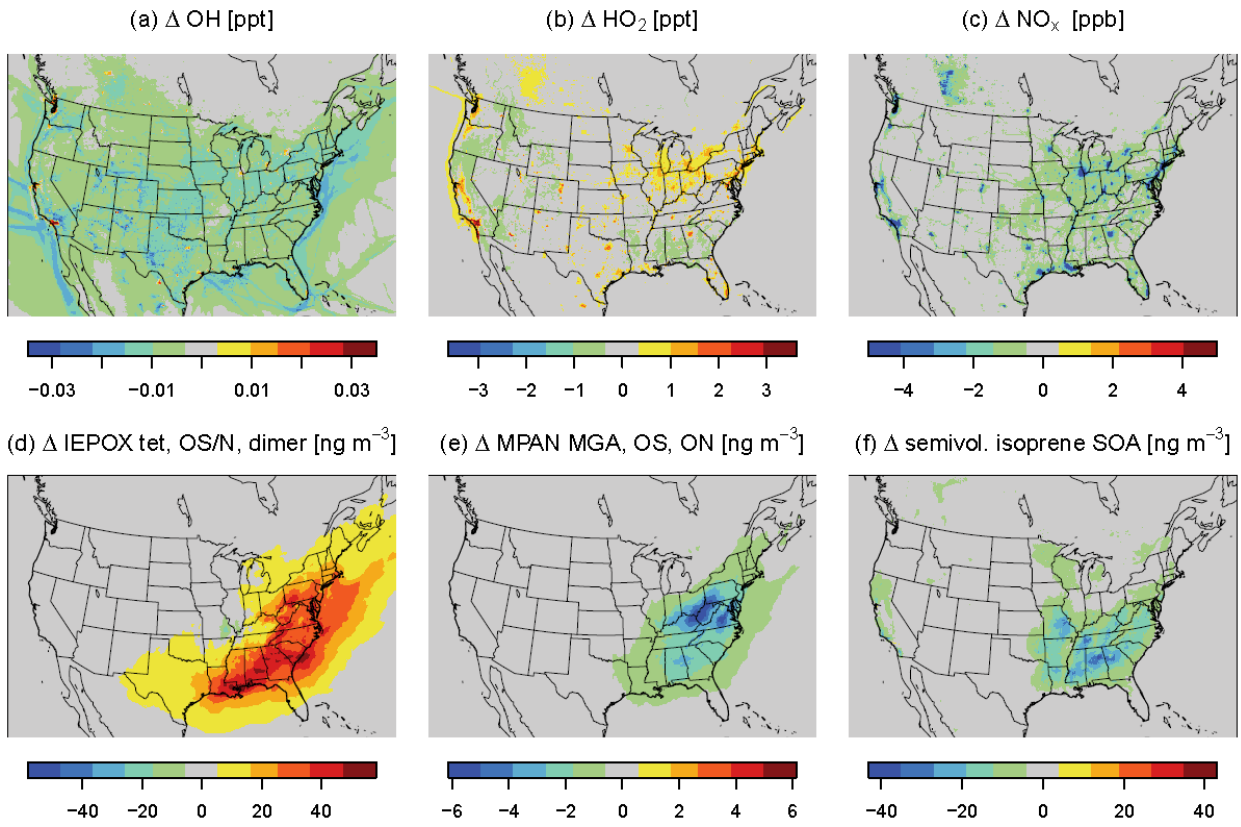

Figure S8: Change in (a) OH, (b) HO_2, (c) NO_x, (d) IEPOX-derived aerosol and isoprene aerosol dimers from all sources, (e) MPAN-derived aerosol, and (f) semivolatile isoprene SOA due to a 25% reduction in NO_x emissions compared to a base simulation for July 2006.

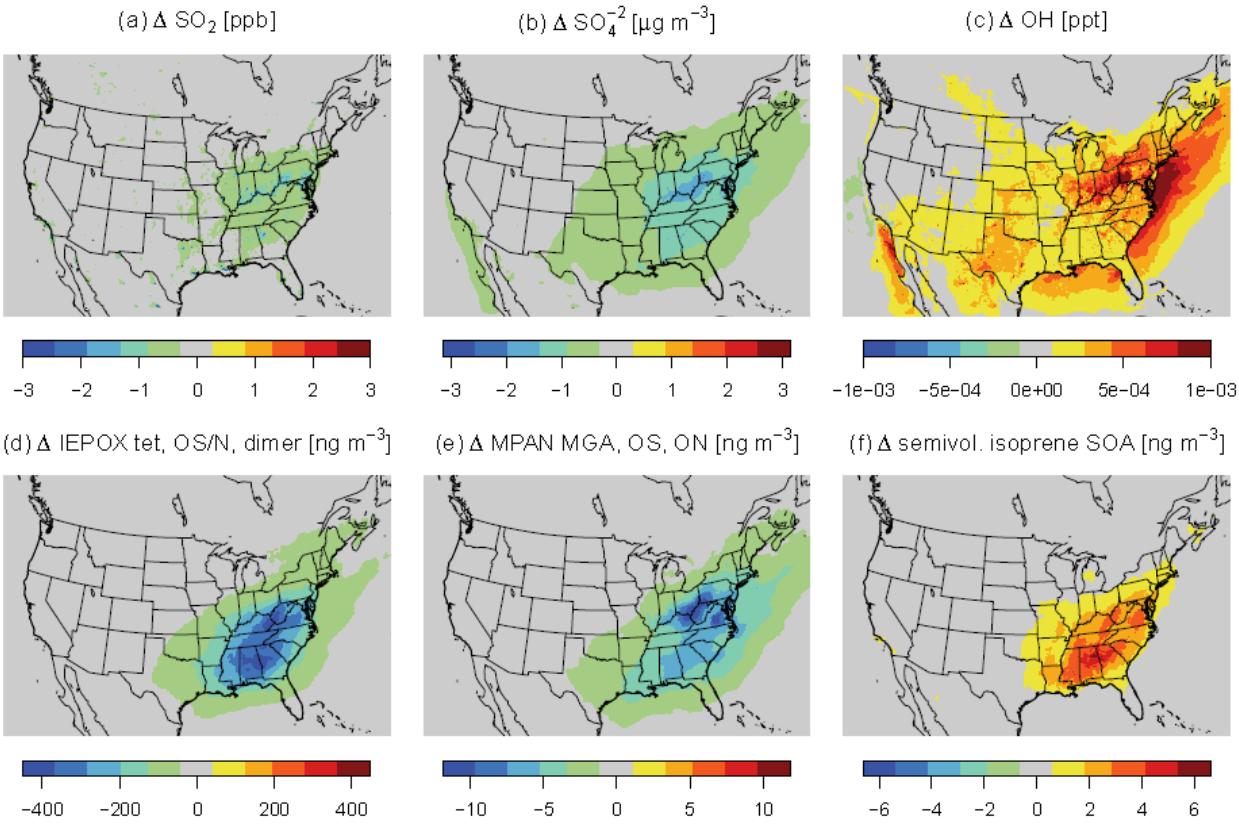

Figure S9: Change in (a) SO_2, (b) sulfate, (c) OH, (d) IEPOX-derived aerosol and isoprene aerosol dimers from all sources, (e) MPAN-derived aerosol, and (f) semivolatile isoprene SOA due to a 25% reduction in SO_2 and sulfate emissions from all sources compared to a base simulation for July 2006.

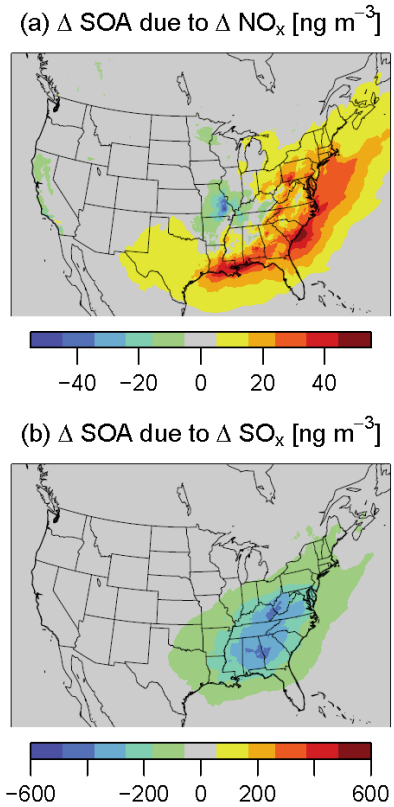

Figure S10: Predicted change in total isoprene SOA (from IEPOX, MPAN, and semivolatile partitioning) compared to a base simulation for a (a) 25% reduction in anthropogenic and wildfire-derived NO_x and (b) 25% reduction in SO_x compared to the base simulation for July 2006.

References

1. Jacob, D. J., Heterogeneous chemistry and tropospheric ozone. *Atmos. Environ.* **2000,** *34* (12-14), 2131-2159.

2. Pleim, J. E.; Binkowski, F. S.; Ching, J. K. S.; Dennis, R. L.; Gallani, N. V., An improved representation of the reaction of N2O5 on aerosols for mesoscale air quality models. In *Regional Photochemical Measurement and Modeling Studies, Vol 2-Results and Status of Modeling*, 1995; pp 904-913.

3. Paulot, F.; Crounse, J. D.; Kjaergaard, H. G.; Kroll, J. H.; Seinfeld, J. H.; Wennberg, P. O., Isoprene photooxidation: new insights into the production of acids and organic nitrates. *Atmos. Chem. Phys.* **2009,** *9* (4), 1479-1501.

4. Eddingsaas, N. C.; VanderVelde, D. G.; Wennberg, P. O., Kinetics and products of the acid-catalyzed ring-opening of atmospherically relevant butyl epoxy alcohols. *J. Phys. Chem. A* **2010,** *114* (31), 8106-8113.

5. Minerath, E. C.; Schultz, M. P.; Elrod, M. J., Kinetics of the Reactions of Isoprene-Derived Epoxides in Model Tropospheric Aerosol Solutions. *Environ. Sci. Technol.* **2009,** *43* (21), 8133-8139.

6. Cole-Filipiak, N. C.; O'Connor, A. E.; Elrod, M. J., Kinetics of the hydrolysis of atmospherically relevant isoprene-derived hydroxy epoxides. *Environ. Sci. Technol.* **2010,** *44* (17), 6718-6723.

7. Renbaum-Wolff, L.; Grayson, J. W.; Bateman, A. P.; Kuwata, M.; Sellier, M.; Murray, B. J.; Shilling, J. E.; Martin, S. T.; Bertram, A. K., Viscosity of alpha-pinene secondary organic material and implications for particle growth and reactivity. *Proc. Nat. Acad. Sci. U.S.A.* **2013,** *110* (20), 8014-8019.

8. Xie, Y.; Paulot, F.; Carter, W. P. L.; Nolte, C. G.; Luecken, D. J.; Hutzell, W. T.; Wennberg, P. O.; Cohen, R. C.; Pinder, R. W., Understanding the impact of recent advances in isoprene photooxidation on simulations of regional air quality. *Atmos. Chem. Phys. Discuss.* **2012,** (12), 27173-27218.

9. Lin, Y.-H.; Zhang, H.; Pye, H. O. T.; Zhang, Z.; Marth, W. J.; Park, S.; Arashiro, M.; Cui, T.; Budisulistiorini, S. H.; Sexton, K. G.; Vizuete, W.; Xie, Y.; Luecken, D. J.; Piletic, I. R.; Edney, E. O.; Bartolotti, L. J.; Gold, A.; Surratt, J. D., Epoxide as a precursor to secondary organic aerosol formation from isoprene photooxidation in the presence of nitrogen oxides. *Proc. Nat. Acad. Sci. U.S.A.* **2013,** *110* (17), 6718-6723.

10. Carlton, A. G.; Bhave, P. V.; Napelenok, S. L.; Edney, E. D.; Sarwar, G.; Pinder, R. W.; Pouliot, G. A.; Houyoux, M., Model representation of secondary organic aerosol in CMAQv4.7. *Environ. Sci. Technol.* **2010,** *44* (22), 8553-8560.

11. Hutzell, W. T.; Luecken, D. J.; Appel, K. W.; Carter, W. P. L., Interpreting predictions from the SAPRC07 mechanism based on regional and continental simulations. *Atmos. Environ.* **2012,** *46* (0), 417-429.

12. Fountoukis, C.; Nenes, A., ISORROPIA II: a computationally efficient thermodynamic equilibrium model for K^+-Ca^{2+}-Mg^{2+}-NH^{4+}-Na^+-SO_4^{2-}-NO_3^--Cl^--H_2O aerosols. *Atmos. Chem. Phys.* **2007,** *7* (17), 4639-4659.